Department of AERONAUTICS and ASTRONAUTICS
STANFORD UNIVERSITY

(NASA-CR-169614) THE 1982 NASA/ASEE SUMMER FACULTY FELLOWSHIP RESEARCH PROGRAM, ABSTRACTS OF RESEARCH PROJECTS, 1ST AND 2ND-YEAR FELLOWS Final Report (Stanford Univ.) 96 p HC A05/MF A01 CSCL 05I G3/80

N83-15163

Unclas 02220

1982

NASA/ASEE SUMMER FACULTY FELLOWSHIP RESEARCH PROGRAM

STANFORD-AMES-DRYDEN FRF

ABSTRACTS OF RESEARCH PROJECTS
1ST AND 2ND-YEAR FELLOWS

TECHNICAL REPORT

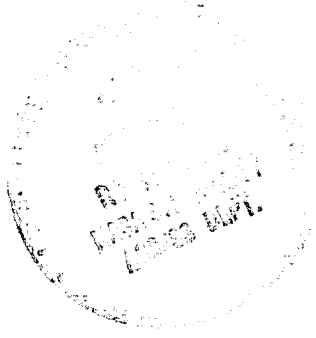

SEPTEMBER 1982

1982

ABSTRACTS

FIRST-YEAR FELLOWS

ASEE Report Summer 1982:

Application of Analytical Redundancy to Failure Detection

Frank J. Alexandro, Jr.
University of Washington

This project was motivated by the problem of detection of sensor failures in a dual tetrad inertial navigation system. The tetrad inertial package consists of four laser gyros, three mounted on orthogonal axes and the fourth mounted at an angle of approximately 54.7^0 to the other axes. The proposed dual tetrad system consists of two tetrad packages mounted some distance apart on an aircraft. Because of the flexibility of the structure and the physical separation of the two tetrad units the gyros and accelerometers do not measure exactly the same quantities. Ames has previously had occasion to study the detection of failures in a single tetrad system (Ref. 1) but analytical redundancy techniques were not used in this study. The term analytical redundancy is usually taken to mean that the dynamic behavior of the system i.e., the differential equation of motion are used as part of the failure detection algorithm.

Several different analytical redundancy systems have been proposed (Ref. 2-5) for use in aircraft guidance system. The basic idea is to use the information about the system dynamics in such a manner that sensor measurements of one quantity can be related via the dynamic equations to quantities measured by other sensors. This is in contrast to what is referred to as hardware redundancy in which multiple sensors measuring the same quantities are used in a "voting" scheme to determine which sensor has failed.

Most analytical redundancy algorithms make use of observers or Kalman filters to compare the information measured by different sensors measuring different quantities in order to detect failures. During this summer I reviewed the available literature on analytical redundancy in an attempt to identify those methods which may be useful for failure detection in a dual tetrad system. Generally the algorithms described are quite complicated and are based on the assumption that the system is linear (or can be adequately described by linearized equations). The effects of nonlinearity, parameter variation and parameter uncertainty have not been extensively considered in published reports. Consequently, it is unclear as to whether it is practical to implement an analytical redundancy scheme in the dual tetrad system. During the coming academic year and next summer I hope to continue to investigate the feasibility of a practical analytical redundancy scheme for a dual tetrad system, and I have submitted a proposal to NASA for graduate student support on this project. During my stay at Ames I have had the benefit of very useful discussions about this project with R. Bach, M. Sidar, and G. Xenakis.

REFERENCES

1. Hruby, R.J.; Bjorkman, W.S.; Schmidt, S.F. and Carestia, R.A., "A Study of Redundancy Management Strategy for Tetrad Strap-Down Inertial Systems", NASA TM #78576, Feb. 1979.

2. Willsky, A.S., "A Survey of Several Failure Detection Methods", Automatica, Nov. 1976.

3. Willsky, A.S., "Failure Detection in Dynamics Systems in "Fault Tolerance Design and Redundancy Management Techniques", AGARD-LS-109.

4. Montgomery, R.C., "Management of Redundancy in Flight Control Systems Using Optimal Decision Theory" in "Theory and Applications of Optimal Control in Aerospace Systems AGARD-AG-251.

5. Deckert, J.C.; et al - "F-8 DFBW Sensor Failure Identification Using Analytic Redundancy", IEEE Transactions on Automatic Control, Vol. AC-22, No. 5, Oct. 1977.

Does Phosphine Photolysis in Jupiter's Atmosphere Lead to Organic Chemical Evolution?

Robert Benson
Nazareth College of Rochester
Assistant Professor of Chemistry

My work, this summer, is part of a long term investigation, At NASA-Ames, into the possibility of organic chemical evolution in Jupiter's atmosphere. These studies have some relevance to the origin of life on earth because the earth's primitive atmosphere may have resembled the present day reducing atmosphere of Jupiter.

Phosphine, PH_3, is a constituent of Jupiter's atmosphere. It has been detected in the region just above the white ammonia cirrus clouds that are a dominant feature of our view of Jupiter. Light from the sun reaching this region is energetic enough to be absorbed by phosphine and cause the photolysis reaction:

(1) $PH_3 + h\nu \rightarrow PH_2 + H.$

The photons absorbed by phosphine contain more energy than is required to break a P-H bond. Most of the excess energy is carried away by the H atom as kinetic energy, producing a so called hot H atom. It is called this because it has more kinetic energy than it would have if it were in thermal equilibrium with the gas.

Hot atom chemistry, or chemical reactions initiated by hot atoms, is a common occurrance in interstellar regions and the upper regions of planetary atmospheres. What I was to investigate was the possibility of the hot H atom initiating organic chemical reactions in Jupiter's atmosphere. In particular , does the abstraction reaction:

(2) $H + CH_4 \rightarrow H_2 + CH_3$ occur producing a methyl radical which can go on to produce more complicated organic molecules?

At the wavelength of light we used 184.9 nm, the hot H atom from phosphine photolysis contains much more energy than is required by reaction 2. However the reaction is not efficient and the hot H atom can become thermalized by collisions and quickly lose its excess energy. Thus it is not at all certain this reaction will occur to any great extent.

The experiment involved mixing accurately known amounts of PH_3, CD_4 and H_2 and exposing the mixture to the 184.9 nm light from a low pressure mercury lamp. CD_4 was used in place of CH_4 because HD will then be formed by reaction 2. Using mass spectrometry to measure the amount of HD formed then gives a measure of the efficiency of reaction 2.

In a simulated Jovian atmosphere consisting of 4 torr PH_3, 20 torr CD_4 and 200 torr of H_2 and a time of exposure resulting in 15 % PH_3 loss - I measured no excess HD formation over the control. A check on the experimental procedure was made by exposing a mixture consisting of 4 torr PH_3 and 320 torr CD_4. In such a mixture thermalization of a hot H atom is less likely to occur before reaction with CD_4. The result was that 0.0088 moles of HD were formed per mole of PH_3 decomposed. This finding indicates

the experimental procedure is working fine.

The more realistic Jovian atmosphere results tell us that phosphine photolysis and the hot H atom produced is not going to lead to the production of methyl radicals by reaction 2. The reason why is probably because H atoms react very readily with PH_3: (3) $H + PH_3 \rightarrow H_2 + PH_2$. This reaction is very close to being diffusion controlled and probably siphons off H atoms.

In summary, my measurement of no abtraction of H from methane, under conditions more favorable for this reaction than on Jupiter, tells us that phosphine photolysis will not initiate organic chemical evolution on Jupiter.

WORKLOAD STUDIES IN AFTI F-16 TEST FLIGHTS

Jan Berkhout, NASA Summer Faculty Fellow
NASA Dryden Flight Research Center, August, 1982

During the summer of 1982 I worked closely with several groups of NASA and Air Force researchers associated with the AFTI F-16 program. The AFTI F-16 incorporates a number of superaugmented and decoupled flight control modes. My aim during the summer of 1982 was to familiarize myself with the flight test program and data collection procedures so that I could obtain and analyze flight data relevant to "pilot work loads" in the superaugmented control modes.

As used by human factors psychologists, the term pilot workload describes an extensive combination of perceptual, cognitive and psychomotor elements (Roscoe, et al., 1978). Work overloads are said to occur whenever anticipated performance requirements might exceed operator capability. A main assumption is that workloads in general ought to be reduced, and that the advantages of any augmented control system should consist at least partly in reduced workload.

Attempts have been made to separate motor and cognitive workload components (Mornay, 1979). In the operation of high performance aircraft a complete separation of the two is not possible or desireable. Complex psychomotor functions do require physical work, and a reduction in the energy demands on the pilot's skeletal musculature often reduces cognitive workload as well.

Psychologists have searched for years for a single parameter measure of workload without success. Workload estimates are necessarily based on a multidimensional array of information. Workload analyses are commonly broken down into four broad categories as follows:

a. Primary task analysis (Chiles and Alluisi, 1979)
b. Secondary (probe) analysis (Ogden et al, 1979)
c. Physiological monitoring (Wierwille, 1979)
d. Subjective reports (Williges and Wierwille, 1979)

These four categories often generate independent and contradictory estimates which are not easily reconciled (Hart et al, 1982). Workload seems to be a genuinely multi-dimensional consruct, and no one category of measures can be adequately interpreted without information from the others as well.

Work load measurements in all four domains are being incorporated into the current AFTI F-16 flight test program. (Crombie and Frazier, 1982). The main interest is, of course, comparing work loads imposed on the pilot when the unconventional control modes are used, and the transition phases from one mode to another. Further on in the test program a number of automated attack and maneuvering systems will be made operational and studied, including voice displays and controls, and the entire rational behind these systems is in fact a reduction of pilot workload.

My main associates during the summer of 1982 were the AFFTC personnel coordinating Human Factors evaluations in the test flight program, particularly Maj. S. Gray and Capt. R. Crombie. P. Sorokowski was my chief contact in the Joint Task Force (JTF) operations office, making flight data available to me, and briefing me on mission scenarios and data formats. The NASA-Dryden researchers in the Dynamics and Control Branch were valuable sources of information on flight dynamics and control theory, particularly P. Carr, and from AFFTC, B. Schofield and T. Twisdale. Finally, on several occasions I was able to meet with Dr. S. Hart at NASA-Ames for discussions on more general applications of work load measurements in aircraft operations.

Primary task analysis. Primary operator outputs in the AFTI F-16 consist of a steady stream of motor activity into four primary flight control axes (Sr; Sp; P and T), the T control being a throttle twist grip not present on conventional aircraft. In some cases the operation of the primary flight controls can be described in terms of continuous operator transfer functions (Heffley, 1982), for which a finite number of gain and phase lag values can be specified. However, in many cases pilot output cannot be adequately specified in terms of continuous transfer functions, and is better handled in terms of Integrated Sequences of Activity (ISAs, Berkhout, 1981), or even as conditioned responses. In such cases the appropriate parameters to monitor would be response time histograms (Berkhout, 1982), or error values relative to information content (Shingledecker et al, 1980).

When closed-loop tasks, such as tracking a known target, are performed an RMS error value can usually be calculated for the concurrent operator transfer functions (Poulton, 1974). For open loop tasks, where target position or the value of disequilibrating inputs are not known, error functions cannot be quantified. However, it is possible to evaluate performance and workload in such cases using spectral density analysis of output in each control channel (Sheridan, 1974), evidence of single channel time sharing (Kinsbourne, 1981), and features of control outputs related to queueing theory (White, 1975). Applications of these techniques to high performance aircraft studies are discussed in Zacharias and Levinson (1979) and Schofield et al, 1982).

My analysis of AFTI F-16 flight data for the initial flights in the program is based on the manual reduction of control force and position values derived from strip charts of telemetered parameters recorded in real time during each flight (Table 1). Epoch boundaries are determined from other flight parameters on these strip charts as shown in Table 1. The value of subsequent work load estimates depends on the correct determination of epoch boundaries, which should indicate such things as the initiation of specific maneuvers, changes in control modes, and arbitrary events associated with maneuvers such as reaching or exceeding certain angles of attack.

Once epoch boundaries have been determined, the strip chart data is examined to establish values of control activity in each discrete axis. This can be done by noting any above-threshold control events, and tabulating reversals of the primary controls. Once this has been done, the activity in all control axes can be collated and examined for evidence of parallel and sequential control outputs. From such data, evidence can assembled concerning the operators control strategy expressed in terms of cycle time, sequence patterns, switching rates and dwell times, and from these data inferences can be drwn concerning the relative work effort across epochs.

In the three flights flown up to August 24, 1982, only the standard normal control mode has been used. Examples of strip chart data are given in Figures 1 - 5, and these indicate that full time sharing of the three primary control axes occured, as would be expected with normal control configuration.

Secondary task analysis. While my main effort this summer has been to set up analysis procedures for the primary control data, information from the other three categories of work load measures will eventually be available as the flight test program proceeds, and will be collated with the primary control output data.

Traditional secondary task analysis includes such "probe" tasks as voice shadowing, reaction time to extraneous stimuli, and mental arithmetic. These are presumed to reflect reserve processing capacity when performed in conjunction with primary control tasks. (Note that only the instructions to the subjects provides the distinction between primary and secondary!) To be effective, the probe tasks ought to impose a constant load at a fixed pace, and meet several other constraints as well (Brown, 1978). For these reasons probe tasks as such have not been included in AFTI F-16 test flights. However, it is possible to regard some forms of voice communications and flight controller instructions as secondary tasks with a precisely defineable information content (Shingledecker et al, 1980). When such communications occur spontaneously during complex test flight scenarios response time and accuracy can be scored, and the impact on primary task functions can be quantified.

Physiological monitoring. Most physiological subsystems show reliable changes with increased cognitive and motor work loads. Under high work load and stress conditions cardiac functions, energy metabolism, blood chemistry and central nervous activity are all rather highly correlated (Berkhout, 1970). Cardiac functions will be monitored on some future AFTI F-16 test flights (Reader, 1981). Basic rate, rate variability and qrs / t wave phase relationships will be recorded. These physiological parameters will be available for correlation with the estimates of work load from the other three categories of data, and will provide a useful interpretive aid.

Subjective workload estimates. There is a large literature of special purpose workload estimation instruments designed for use with high performance aircraft operations, which combine multi-attribute theory and scaling techniques to produce equal-interval response matrices for grouped pilot responses (Donnell and O'Conner, 1978; Reid et al, 1981; Williams, 1982). These response measuring instruments are in theory to the traditional ordinal scales of aircraft handling qualities such as the Cooper-Harper (1969), a ten rank rating list. The best of these multi-attribute instruments unfortunately require a large amount of interviewer-pilot contact time, and a pool of group data. Both these requirements are unrealistic in terms of the AFTI flight test program constraints. The emphasis in AFTI debriefing will be on segregating pilot workload estimates for single mission phases (Greene et al, 1981) rather than obtaining load estimates for larger mission segments. The methodological emphasis will be on obtaining a true, discrete boundary for the desired event or control condition, which may be quite brief.

Continuation studies. As more test flights are completed, Major Gray and Mr. Sorokowski have agreed to send copies of the appropriate strip charts containing pilot control outputs to me at the Human Factors Laboratory at the University of South Dakota. Further analysis of the strip chart data will continue during the academic year 1982-1983 along the lines indicated above. While I will be concentrating on primary task data, information concerning work load estimates for the same flight epochs but derived from the other three categories will be made available for correlation with the primary output data. The primary data analysis is generally based on an open-loop interpretation of the test flight scenario. Closed-loop data may become available later in the flight program when tracking scores for HQDT or "aggressive tracking" become available, and workload scores can be collated with tracking values. In particular, the early flight data must really be considered baseline data, since the augmented control modes and the fourth control axis have not yet been used. Operator output bandwidth, channel capacity and queueing of output elements will be of much more interest in the four axis augmented modes.

Apart from the further processing of strip chart data several other procedures for analyzing AFTI F-16 workload levels are possible. Power spectral density and cross-spectral transformations of the motor output time series would permit a more precise look at bandwidth and shared power aspects of multi-axis tracking. Once available, these transformations can also be used for calculating event-linked postgrade and retrograde averaging of control operations. In such a data reduction, the "events" would be critical points in the flight scenario, and the averaged responses would show such things as the time needed to damp out responses in particular frequency bands.

Once the magnitude and quality of data generated by the AFTI F-16 test flight program is known in more detail, I will present a proposal for NASA support of further work, along the lines suggested in the paragraph above, to be done at the Human Factors Laboratory at the University of South Dakota, and involving approximately 12 man-months of data analysis effort by senior graduate students in the doctoral program in human factors.

REFERENCES

1. Berkhout, J. Psychophysiological Stress: Environmental factors leading to degraded performance. IN: DeGreene, K.B., (ed.) Systems Psychology, McGraw-Hill, NY, 1970, pp 407-450.

2. Berkhout, J. Sources of inter-individual differences in the perceived difficulty of F-18 pilot subtasks according to mechanisms of learning and execution. Final Report, Contract N00123-79-C159, PACMISTECEN. Human Factors Laboratory, University of South Dakota, Vermillion SD, April, 1981.

3. Berkhout, J. Incorporation of Human Performance Measurement Capability in the NADC Crest Simulator Facility. NADC, Warminster PA. Technical Report, June, 1982

4. Brown, I. D. Dual Task Methods of Assessing Workload. Ergonomics, 21:3, 1978, 221-224.

5. Chiles, W. D., and Alluisi, E. A. On the Specification of Operator or Occupational Workload with Performance Measurement Methods. Human Factors, 21:5, 1979, 515-528.

6. Cooper, E. and Harper, P. The use of pilot rating in the evaluation of aircraft handling qualities. AGARD report #567, Paris, April, 1969.

7. Crombie, R. B. and Frazier, M. L. The AFTI-F16 flight test program and opportunities to evaluate pilot-vehicle interface and mission effectiveness. AFFTC Technical Report No. 82-30, Edwards AFB, 1982.

8. Donnell, M. L. and O'Conner, M. F. The application of decision analytic techniques to the test and evaluation phase of the acquisition of a major air system. Technical Report #TR 78-3-25. Decisions and Designs, Inc., McLean VA, April, 1978.

9. Greene, J. H., Arbak, C. J., Courtright, J. F., and O'Donnell, R. D. Ground Attack Tactics Survey (GATS) AFAMRL TR-81-68, Wright-Patterson AFB, 1981.

10. Hart, S. G., Childress, M. E., and Hauser, J. R. Individual Definitions of the Term "Workload". NASA Ames Research Center, Personal Communication, 1982.

11. Heffley, R. K. Pilot Models for Discrete Maneuvers. Technical Report, Systems Technology Inc., Mountain View, California, 1982.

12. Kinsbourne, M. Single-Channel Theory. In: Holding (ed), Human Skills, Wiley, NY, 1981, pp 65-90.

13. Mornay, N. (ed), Mental Workload, its Theory and Method. Plenum Press, NY, 1979.

14. Ogden, G. D., Levine, J. M. and Eisner, E. J. Measurement of Workload by Secondary Tasks. Human Factors, 21:5, 1979, pp529-548.

15. Poulton, E. C. Tracking Skill and Manual Control. Academic Press, London, 1974.

16. Reader, D. C. Physiological and Performance Parameters as Indices of Pilot Workload. An Analysis of Data from the AFTI-F16 Project. AFTI-F16 Project Memorandum, USAF School of Aerospace Medicine, Brooks AFB, 1981.

17. Reid, G. B., Shingledecker, C. A. and Eggemeier, F. T. Application of Conjoint Measurement to Workload Scale Development. Proceedings, Human Factors Society 25th Annual Meeting, Rochester, NY, 1981.

18. Roscoe, A. H., Ellis, G. A. and Chiles, D. Assessing Pilot Workload. NATO AGARDOGRAPH AG-233, Neuilly-sur-Seine, 1978.

19. Smith, B. L., Twisdale, T. R., Kitto, W. G. and Ashurst, T. A. Development of Handling Qualities Testing in the 1970s: A New Direction. Project Memorandum, NASA Dryden FRC, 1982.

20. Sheridan, T. B. and Ferrell, W. R. Man-Machine Systems. MIT Press, Boston, 1974. pp 247-258 (Chapter 12: Optimal control models using state variable concepts)

21. Shingledecker, C. A. and Courtright, J. F. Subsidiary Radio Communications Tasks for Workload Assessment in Simulations. Technical Report No. AFAMRL TR-80-126, Wirght-Patterson AFB, 1980.

22. White, John A. Analysis of Queueing Systems. Academic Press, NY, 1975.

23. Wierwille, W. W. Physiological Measures of Aircrew Workload. Human Factors, 21:5, 1979 pp 575 - 594.

24. Williams, K. N. Assessment of Reliability and Validity for the Systems Operability Measurement Algorithm (SOMA) AFTI-F16 Project Memorandum, PACMISTECEN, Mt. Mugu CA, 1982.

25. Williges, R. C. and Wierwille, W. W. Behavioral Measures of Aircrew Mental Workload. Human Factors, 21:5, 1979.

26. Zacharias, G. L. and Levison, W. H. A performance Analyzer for identifying changes in Human Operator Tracking Strategies. AMRL TR-79-17 WPAFB, March 1979.

Infrared Observations of M17

Elizabeth Brackmann

State University of New York at Stony Brook

There is increasing observational evidence that massive stars tend to form near the edges of dense clouds of gas and dust in the galaxy, leading to the formation of "blisters" of ionized hydrogen at the surface of the clouds. This summer I have studied infrared emission from one of the most energetic of these star forming complexes, M17. Attention has been focused on the properties of the emission at 20, 50, and 100 microns, on the temperature distribution of the IR emitting dust, and on the role of several stellar-like point sources recently discovered in the near-IR by Ames observers in the overall energy balance of the region. The results of this analysis have been combined with the work of past investigators who have studied other aspects of M17-- its stellar populations, radio emission from diffuse and compact regions of ionized hydrogen, millimeter wavelength observations of molecules deep in the cloud core and IR emission at other wavelengths and resolutions-- to refine our view of ongoing star formation in this region. A paper is now being prepared on this work in collaboration with Mike Werner of the Space Sciences Division.

The initial analysis was done using the high resolution (30 arc seconds) data at 50 and 100 microns taken with the Kuiper Airborne Observatory. Dust temperatures were derived by fitting a black body temperature curve to the 50 and 100 micron emission at each measured point and then correcting for a dust absorbing efficiency which goes as $1/\lambda$. The temperature decreases steeply from east to west. Comparison of the 100 micron brightness with that estimated for a blackbody at the observed 50-100 micron color temperature indicates that the opacity increases steeply to the west. In addition, the 50 and 100 micron emission maxima are displaced from one another in the direction of the steepening density gradient. The most likely interpretation of these results is that a high extinction cloud is heated from its eastern side by young stars located near its edge. The longest wavelengths penetrate the furthest into the cloud with the least ability to heat dust, hence the warmer (50 micron) dust lies closer to the heating source than the cooler (100 micron) dust.

This model is an extension of the picture proposed by other observers. The 6 cm radio emission from ionized hydrogen adjacent to the far-infrared peaks has been interpreted as the front between the HII region and the molecular cloud seen edge on. The present results depart from previous work in showing that the peak IR luminosity in the molecular cloud is too bright and compact to be heated by the star clusters to the east which are thought to power the HII region. My hypothesis is that there

is a deeply embedded unobservable star cluster closer to the IR peak providing local heating. The newly discovered near-IR point sources lie in the predicted location for the new heating source. Examination of the spectrophotometry of the 14 near-IR sources shows that they are very luminous but cool (100°K) objects, most likely massive young stars (30,000°K) throwing off dust shells heated to 100°K. The heated shells may be the only evidence of other nearby young stars without heated shells, but highly obscured by foreground dust, whose unbounded radiation is powering the local area. Work is now in progress on the other possible interpretations of the near-IR point sources.

One of my main motivations for coming to Ames this summer was to become more familiar with the techniques of IR instrumentation and data handling. I have had several usefull demonstration-discussions with my NASA colleague Tom Roellig on the state-of-the-art research being done in his lab (NASA-Ames Space Sciences Division) on low temperature high sensitivity IR detectors. During the summer I also spent a substantial fraction of my time reducing the data for a very high resolution (5 arc second) 20 micron map of M17. The data was taken using a beam-switching mode in which a position is sampled at the same time as adjacent positions a few arc seconds on either side. When the adjacent measurements are of blank sky they provide an easy means of removing atmospheric contributions from the signal at the central point. In this case adjacent measurements were taken within the Ir emission region and a scheme had to be devised to deconvolve true signal from the relative measurements at each point. The final 20 micron map shows a number of peaks in addition to an extended background which is co-extensive with 6 cm radiation from the ionized hydrogen at the edge of the cloud. The 20 micron peaks coincide with compact HII regions and with some of the near IR point sources and have been useful in determining the nature of the new embedded cluster.

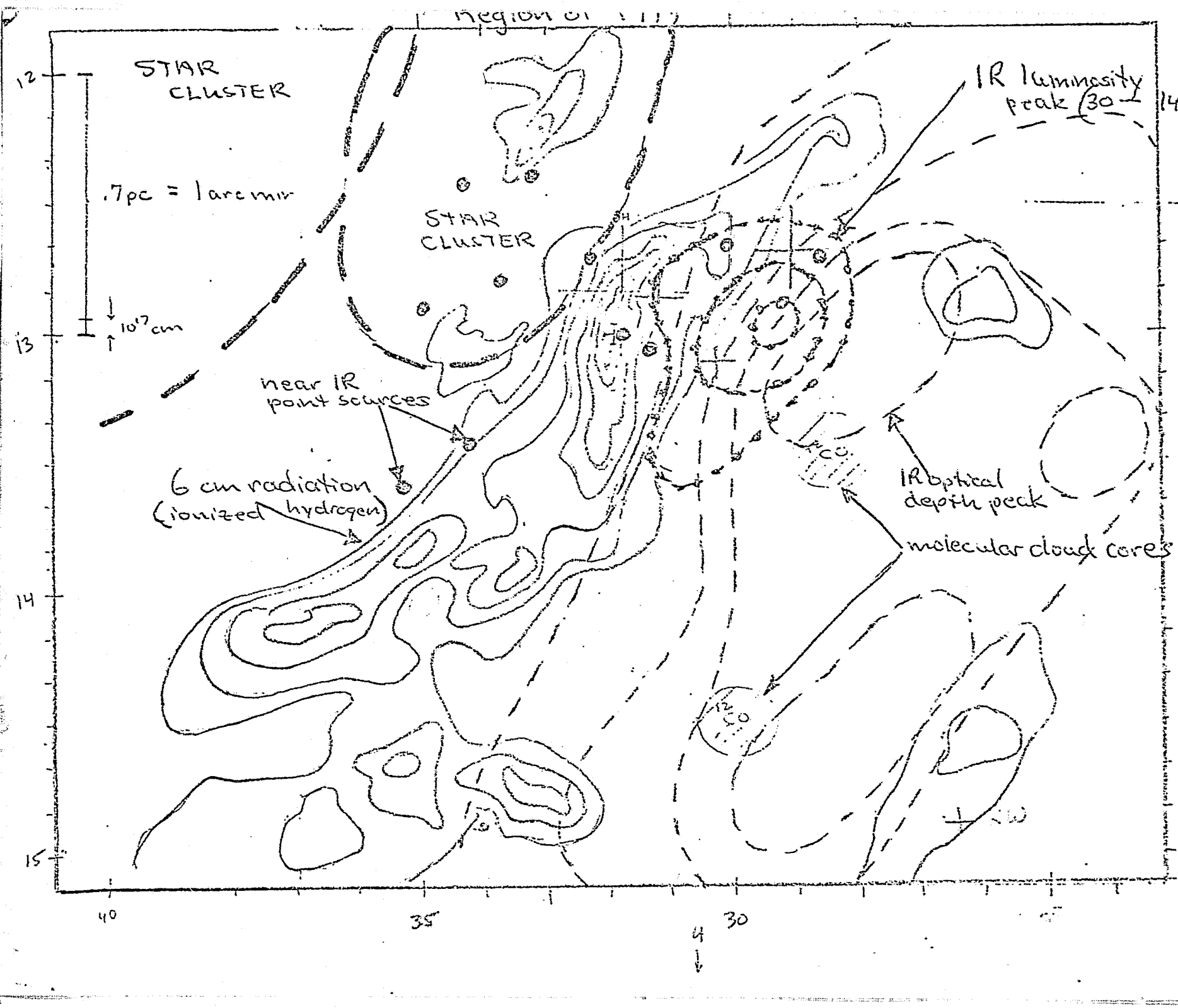

1. ANALYSIS OF TWO-WAY CONTINGENCY TABLE BY ROCK AND VEGETATION TYPES

2. MODIFIED MAXIMUM LIKELIHOOD CLASSIFICATION PROCEDURES AND THEIR APPLICATION TO PATTERN RECOGNITION IN REMOTE SENSING

Hubert J. Chen
Department of Statistics and Computer Science
University of Georgia

1982 ASEE Summer Research Fellow
Stanford University and NASA/Ames Research Center

Dr. David Mouat at the Technology Applications Branch is currently conducting a research project in geology on determining the relation between rock and vegetation types. The sampling survey and statistical analysis are to be used as basic tools for the study. It is suggested that a minimum sample of 250 items for the ten by five contingency table be collected by a random process. It is also suggested that a large sample be considered if more budget funds and time are allowed.

Due to possible empty cells in the contingency table, the actual statistical analysis could be more complicated. Empty cells occur in two situations: (1) when the sample size is not large enough (small sample effect), and (2) when the cell combinations are impossible (with probability zero cells). A resolution for the former case is to add a small number, say 0.5 or 1 to every cell and then the usual chi-square test for independence (or equivalently, no interaction) could be employed [4]. In addition, a log linear model via logorithmic transformation of the expected frequency may be used to convert this table into a two-way ANOVA type problem. Thus, Tukey's one-degree-of-freedom test for interaction is possible and furthermore, test and comparisons among row/column effects can be made. For the latter case the with-probability-zero cells cannot be adjusted or estimated; a special method through iterations must be used to derive the expected frequencies for the nonempty cells. Then, a chi-square test for the quasi-independence can be performed [1]. Further analysis can also be made by a log transformation for all nonempty cells. In this situation an ANOVA test is possible using regression model via the use of SAS statistical package [5] in which sum of squares type I, II, III and IV should be read and interpreted with caution.

The second problem I have been working on is pattern recognition in remote sensing via a satellite, which was hinted by Dr. Don Card of the Technology Applications Branch, NASA/Ames Research Center. This subject interests me a lot. A modified maximum likelihood classifier which should have the potential of increasing the accuracy of classification is studied.

At the present time statistical model used to classify a picture element (pixel) on earth into an appropriate category of land cover and land use is a multivariate normal probability distribution on the brightness values or color-coded values $(X_1, X_2, \ldots, X_p)$ collected and digitized by multispectral scanner system (MSS) installed in a land satellite [3, 6]. The domain of the model which is assumed to be in the entire multidimensional space may

not reflect the practical situations. Instead, it is more likely to be restricted in certain finite intervals say (a,b). The brightness values from a spectral band, for example, are confined in the range of (0, 127) in an MSS of Landsat. Based on this reason a doubly (two-sided) truncated multivariate normal probability model is assumed on the vector $(X_1, X_2, \ldots, X_p)$; and the conjecture is that based on the truncated model the accuracy of classification of a pixel into a class could be increased using maximum likelihood classification principal.

Since the true parameters of the probability model are generally unknown, one has to estimate them using training samples of known features on the ground. To do this the maximum likelihood method or moment method can be used [2, 4]. As a result, a system of simultaneous $p(p+3)/2$ nonlinear equations must be solved by high speed computers. A generalization of the model to several classes with different mean vectors but with the same covariance structure will be investigated in the future. Comparisons between nontruncated and truncated probability models will be made accordingly in terms of the chance of misclassification.

References

[1] Everitt, B. S. (1977). The Analysis of Contingency Tables. John Wiley & Sons, Inc., New York.

[2] Gupta, A. K. and Tracy, D. S. (1976). Recurrence relations for the moments of truncated multinormal distribution. Commun. Statist. Theor. Meth. A5(9), 855-865.

[3] Lillesand, T. M. and Kiefer, R. W. (1979). Remote Sensing and Image Interpretation. John Wiley & Sons, Inc., New York.

[4] Ratani, R. T. and Gajjar, A. V. (1977). Estimation of parameters of a truncated multivariate normal distribution. South African Statist. J. 125-137.

[5] SAS79. A Statistical Analysis System. SAS Institute, N. C.

[6] Swain, P. H. and Davis, S. M. (1978). Remote Sensing: The Quantitative Approach. McGraw-Hill, Inc., New York.

Facilities for Simulation of OTV Aerothermodynamics

Dick Desautel
Associate Professor,
Mechanical Engineering
San Jose State University

My summer project has consisted of developing an understanding of the problem posed of experimentally simulating orbital transfer vehicle (OTV) aerothermodynamics. The proposed OTV mission involves a unique flight regime for the dominant aerodynamics and heat transfer. This flight regime is one of hypersonic (18 to 37 for M), low density (Kn = 0.001 to 0.3), and intermediate Reynolds Number (10 to 100,000) flow. The flow is dominated by real gas effects and and nonequilibrium conditions due to the high total enthalpy. This regime has been encountered on previous missions, but has never been the sole regime in which the vehicle experiences the significant atmospheric effects. The summer's project addressed the question: What is the experimental aerothermodynamic simulation problem posed by this mission and how should we go about solving it? It will be recognized that the state of knowledge concerning gas kinetics, gas dynamics, and gas chemistry is far from adequate in the hypersonic, low density regime, and hence there is a strong motivation for achieving experimental simulation of the aerothermodynamics.

During work on the project, I reviewed the literature, both on fundamentals and on applications, of impulse-type flow facilities with emphasis on shock tube derived facilities. I also interacted strongly with Dr. Chule Park to gain insight into particular advantages/diadvantages of each device, and pragmatic performance capabilities. At the same time, I studied the basic concepts of similitude as applied to the hypersonic and low density (rarefied) gas regimes.

A further background investigation considered the rationale for OTV flight regime and its consequent free-stream flow parameters.

All this background and developing familiarity with the problem was synthesized and a simulation strategy evolved. The project's conclusions were primarily that separate simulations of flow field (aerodynamics) and the relevant gas kinetics/chemistry were needed, the former involving at first simple glow-discharge diagnostics in a simple shock tunnel and the latter involving long-term commitment to proper modification of existing shock tube facilities to produce the required gas purity and total temperature.

"Model Reduction Methods for Maneuver Autopilot Design"

Kenneth Dunipace

Indiana University - Purdue University at Indianapolis
Professor of Engineering

The Problem:

Linear dynamic models of aircraft and other complex systems are often represented by a high-order differential equation. Such models are ususally derived from complicated analytical design procedures and involve predicted values of numerous system parameters. The complexity of such models provide a serious handicap to understanding system behavior. Similarly, the cumulative effect of uncertainties in predicting parameter values lead to gross inaccuracy and misleading characteristics in the high order models. In addition, low-order models are reported to be important in the design of robust controls.

The objectives of this project is to develop useable and reliable procedures for extracting from a high-order model those lower order models which retain the essetial dynamics of the real system and provide desireable insight or design properties. Such procedures would be of current value in the design of control laws for the Maneuver Autopilot being used in the Hi-Mat aircraft. They will be of similar value in implementation of control laws for future application of the Maneuver Autopilot concept.

Status:

During this summer, I have initiated a literature review, applied each of four different methods to a simple example system to illustrate the functioning of the method. In addition, I have spent time learning to use the Cyber Interactive Facility and the ORACLS subroutines in applying the methods studied and in analysing methods still to be considered.

Literature Review:

At present, I have obtained ten technical reports dealing with different methods of model reduction. These reports include references to additional reports. Thus, there seems to have been a significant amount of study on this subject. I expect to continue my review of existing methods.

Three of the methods presented (FERNANDO, MOORE, and PERNEBO) are applied to systems which have previously been "balanced". The concept of "balancing" is presented by Moore. His report was one of the first obtained and I have spent much of the summer developing the algorithm and associated computer program to perform the balancing procedure. The "balancing" procedure may be intrinsically valuable as it is claimed to lead to a robust form of control law.

Moore's report contains 31 references, some of which should be reviewed for additional information. The report also contains numerous proofs to support the development of the concept and several examples of its application. The Moore method of reduction is one of the four which I have illustrated by example.

Due to the large amount of time spent extracting the "balancing" algorithm and developing the computer program to implement the algorithm, I have not yet reviewed the other two methods applied to the "balanced" system (FERNANDO, PERNEBO).

A recent report (GUTMAN) describes a rather simple method based on differentiation of polynomials. It was selected for review because it was simple and I needed material for my mid-summer presentation. It is one of the four which I have illustrated by example. In its present form it applies only to single-input single-output systems. An extension to the multi-variable case should be considered.

In a recent study (WALKER) for DFRF, a method described as "residue retention" is used as part of the process of obtaining a reduced model of the combined system composed of the aircraft and the pilot. In this study, the 31st order model is reduced to a sixth-order model. It isn't clear whether this method was originated by Walker of developed form another report (SKELTON). While a lot of time was spent studying the Walker report and the "residue retention" method. This method is one of the four which I have illustrated by example. It has the undesireable property of introducing spurious high frequency zeroes into the reduced system transfer function. I have not reviewed the Skelton report, but expect that such a review will clarify the origin of the "residue retention" method.

The fourth method illustrated by example was called "State Variable Observation" and is simply a state-variable representation of the "Dominant-Root Concept" presented in elementary control textbooks (e. g. DORF).

The other reports (EL-ATTAR, KOKOTOVIC, KRISHNAMURTHY, and SHAKED), which have not been reviewed, are listed in the bibliography.

The Example System:

The example system, used to illustrate each of the methods, is:

$$T(s) = 0.48(s+3)(s+5)/(s+1)(s+2)(s+6)$$

This system has an impulse response of:

$$y_s(t) = 1.54e^{-t} - 1.08e^{-2t} + 0.024e^{-6t}$$

and a step response of:

$$y_a(t) = 1 - 1.54e^{-t} + 0.54e^{-2t} - 0.004e^{-6t}$$

The system was chosen because, clearly, the response due to the eigenvalue at -6 contributes little to the response and the system does have a good lower-order model. Hence it should be effective in displaying the performance of various methods. A set of view-graphs was prepared comparing state variable models, transfer-function models, impulse responses, and step responses of this system using the classical "Dominant Root." method (DORF) and each of the four methods described above.

Due to space limitations, only the step responses are presented in summary:

A. Dominant-Root:

$$y_a(t) = 1 - 1.54e^{-t} + 0.54e^{-2t}$$

B. State Variable Observation:

$$y_a(t) = 1 - 1.54e^{-t} + 0.54e^{-2t}$$

C. Residue Retention:
$$y_m(t) = 1 - 1.53e^{-t} + 0.53e^{-2t}$$

D. Differentiation of Polynomials:
$$y_m(t) = 1 - 1.24e^{-1.25t} + 0.24e^{-3.19t}$$

E. Moore method:
$$y_m(t) = 0.78 - 1.14e^{-1.02t} + 0.362e^{-1.90t}$$

State Variable Recovery:

Most of the methods of model reduction involve similarity transformation of the system model. Thus, the reduced model is expressed in terms of state variables which differ from those of the original system model. If, as is usually the case, the variables in the original model are physical variables of real interest, then a method must be derived to recover the original states from the reduced states. The similarity transformation cannot be reversed because of the reduction. As an initial attempt at solving this problem, I developed a program which reduces systems which have been "balanced" and then recovers a least-squared estimate of the original states. While the method works mathematically, it does not seem to produce physically reasonable results. Further study is needed.

Bibliography:

DORF: Richard C. Dorf, "Modern Control Systems", Addison-Wesley, 1980

EL-ATTAR: R. A. El-Attar and M. Vidyasagar, "Order Reduction by l1 and l∞ Norm Minimization", IEEE Transactions on Automatic Control, Vol. AC-23, No. 4, Aug. 78, pp 731-733

FERNANDO: K. Vincenza Fernando and H. Nicholson, "Singular Perturbational Model Reduction of Balanced Systems", IEEE Transactions on Automatic Control, Vol. AC-27, No. 2, Apr. 72, pp 466-468

GUTMAN: Per-Olof Gutman, Carl Frederick Mannerfelt, and Per Molander, "Contributions to the Model Reduction Problem", IEEE Transactions on Automatic Control, Vol. AC-27, No.2, Apr. 82, pp 454-455

KOKOTOVIC: P. V. Kokotovic, R. E. O'Malley, and P. Sannuti, "Singular Perturbations and Model Reduction in Control Theory - An Overview", Automatica, Vol.12, 1976, pp123-132

KRISHNAMURTHY: V. Krishnamurthy and V. Seshari, "Model Reduction using the Routh Stability Criterion", IEEE Transactions on Automatic Control, Vol. AC-23, No.4, Aug. 78, pp729-731

MOORE: Bruce C. Moore, "Principal Component Analysis in Linear Systems: Controllability, Observability, and Model Reduction", IEEE Transactions on Automatic Control, Vol. AC-26, No. 1, Feb. 81, pp382-387

PERNEBO: Lars Pernebo and Leonard M. Silverman, "Model Reduction Via Balanced State Space Representations", IEEE Transactions on Automatic Control, Vol. AC-27, No. 2, Apr. 82, pp 382-387

SHAKED: U. Shaked and N. Kartanias, "The Use of Zeros and Zero-Directions in Model-Reduction", International Journal of Control, Vol. 23, No. 1, 1976, pp 113-115

SKELTON: Robert E. Skelton, "Cost Decomposition of Linear Systems with Applications to Model Reduction", International Journal of Control, Vol. 32, No. 6, 1980, pp 1031-1055

WALKER: Robert Walker and Naren Gupta, "Flight Test Trajectory Control Analysis", ISI Report 16, May 82 (unpublished)

Microbial and Nutrient Analyses in Controlled Environmental Support Systems for Plants

Diane Dudzinski
Professor of Biology
College of Santa Fe

If higher plants are to be used to supply food, oxygen and potable water as life support for man during large scale manned space missions, then it seems reasonable to assume that bacterial accumulations will occur within such systems. These potential contaminants can enter via the air, the nutrient medium, man and plants. They may have harmful and/or beneficial effects depending upon the species. Therefore, it may be necessary to control microbial populations within such systems. In addition if nutrient solutions are to be recycled within such systems, it may be necessary to know at what rate specific nutrients are depleted from the system for different plants.

Steve Schwartzkopf of NASA/AMES has developed a computer monitored closed plant chamber which can precisely monitor and control a number of physical and chemical gas parameters. I came to NASA/AMES this summer to work with Steve Schwartzkopf and Robert McElroy in the CELSS program, and to investigate the above mentioned problems.

Experiments run this summer include the growth of 'Grand Rapids' lettuce from seedling to harvest in an open environmental plant chamber over two, four week periods. During these experiments bacterial and nutrient samples were periodically collected for analyses. During the first four week period a UV lamp was continuously "on", and during the second four week period a UV lamp was continuously "off". In another experiment involving the closed plant chamber, a tomato plant was placed into the chamber and samples were periodically taken for bacterial and nutrient analyses.

All microbiological media, supplies, incubators, Quebec colony counters, plant growth chambers as well as atomic absorption spectrophotometer and reagents for nutrient analyses were supplied by NASA.

Bacterial findings to date show that UV light emitting wavelengths of 245 nm can reduce bacterial populations from 60,000 cells per ml. to less than 200 cells per ml. within 24 hrs. per 100 liters of nutrient solution having a flow rate of 20 l. per min. (see FIGURE 1). Bacterial species identified within the chambers include pathogenic Staphylococci spp., Erwinia sp.; opportunistic microbes such as Pseudomonas spp., Chromobacterium sp., and other microbes such as Lactobacillus sp., Acinetobacter spp., Sphearotilus natans, Leptothrix sp., Serratia liquefaciens and Alcaligenes sp.. Several of the species identified are involved in the production of ethylene and other gases as well as toxins and could be considered phytopathogens. Nutrient analyses to date are incomplete, but do suggest that metals such as iron are rapidly depleted from the nutrient medium and may be complexed as precipitates onto the sheaths of Sphaerotilus natans and/or Leptothrix sp. Completion of the analyses from these experiments will be undertaken at the College of Santa Fe during the year.

If funding is approved for a second summer as a NASA/ASEE, I would like to examine the same parameters under intermittent UV light exposure which may be more energy efficient and just as effective in controlling microbial populations. In addition I would like to examine interactions between higher plants, algae and microorganisms within a closed environmental chamber.

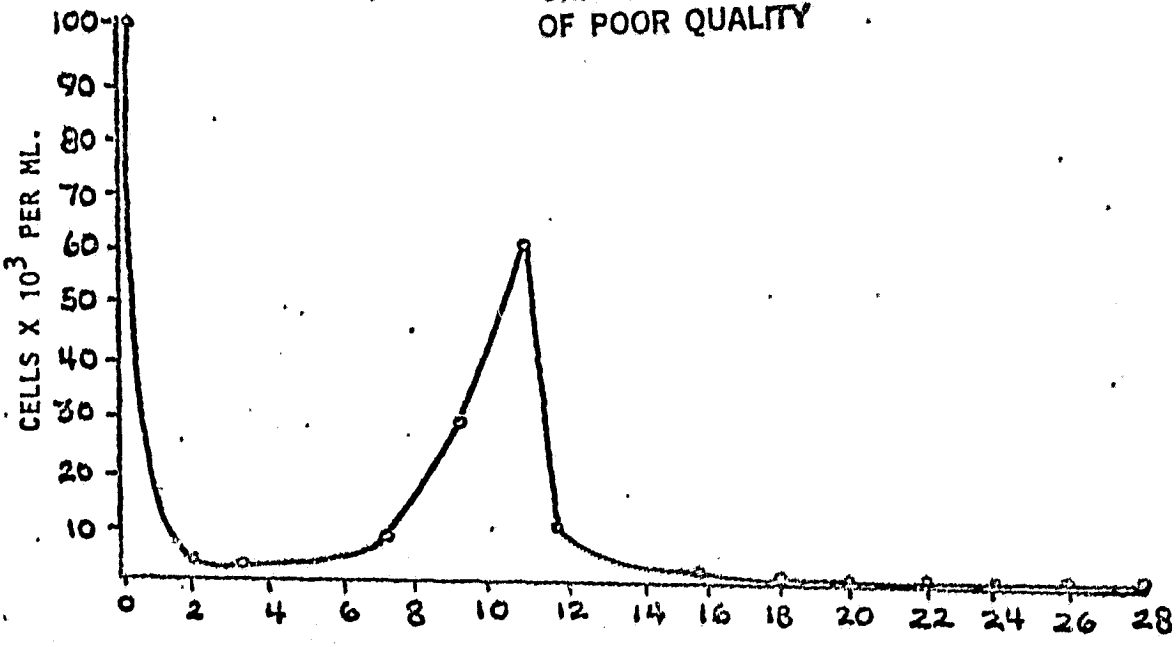

OPEN HYDROPONIC PLANT CHAMBER WITH UV LIGHT ON

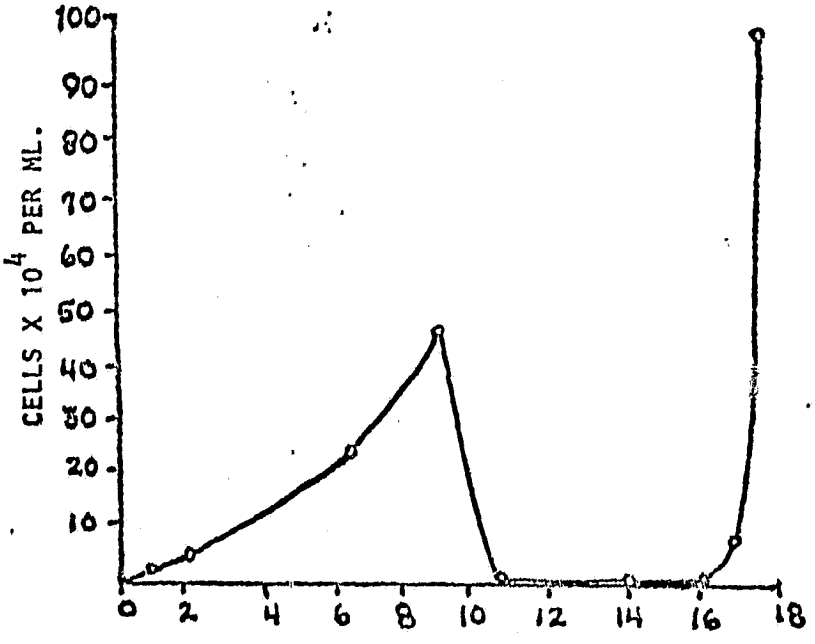

CLOSED AEROPONIC PLANT CHAMBER WITHOUT UV LIGHT

FIGURE 1. Microbial cell numbers in controlled environment plant chambers.

REFERENCES

1. Buyanovsky, J. and Gale, J. 1981. Ultraviolet Radiation for the Inactivation of Microorganisms in Hydroponics. Plant and Soil 60, 131-136.

2. Hammer, P. A., Tibbitts, T. W., Langhams, R. W.,,and McFarlane, J. C. 1978. Base-line Growth Studies of 'Grand Rapids' Lettuce in Controlled Environments. Amer. Soc. Hort. Sci. 103(5):649-655.

3. Maguire, Jr., B. 1980. Literature Review of Human Microbes Interaction with Plants. NASA Contractor Report 166330.

THE PAY-OFF OF HIGH LIFT

Donald L. Elder

San Jose State University
Lecturer in Aeronautics

This project was to examine the potential benefits of further developments in the area of conventional mechanical high lift aerodynamics for subsonic aircraft. Power augmented lift was excluded. This topic was suggested by NASA colleagues V. Corsiglia and Larry Olson.

The approach taken was to review the literature for the state of the art in aerodynamic high lift technology, for aircraft design optimization with respect to high lift and for the economics of aircraft operations with respect to the significance of high lift capabilities and then to draw some inferences as to the improvability potential and the cost/benefit aspects of advanced high lift performance.

NASA/AMES is a good location to carry out this investigation because of the key research being done here along with the excellent library/search facilities. Theory, powerful computerized analytical methods and outstanding research test facilities were found to be producing exciting advances in high lift. NASA sponsored studies by aircraft industry contractors produce excellent independent assessments of the state of the high lift art and its appropriate applications to the aviation field. Included in this review were studies by NASA and contractors of High Performance Single Engine Airplanes, Applications of Advanced Technologies to Small Short Haul Aircraft, Applications of High Technologies to Commercial Advanced Designs and High Lift Concepts Selected for the Energy Efficient Transport Program.

Aerodynamic theory suggests that today's maximum lift and lift-to- drag ratios could ideally be doubled or more. Nearly half of what can be demonstrated on an experimental basis for two-dimensional flow is lost when applied to a complete aircraft. Nevertheless, great advances are being made in increasing two-dimensional high lift. The heretofore unusable region beyond the onset of wing flow separation may now become part of the designer's province for tailoring an optimal aircraft design. Normally unacceptable flying qualities near, at and beyond the stall have resulted in conservative Federal regulations which effectively prohibit utilization of from thirty to forty per cent of the available well behaved upper portion of the presently demonstrated high lift capability.

A spectrum of aircraft types and operations were examined which included single engine high performance personal/business aircraft, small multi-engine executive/business aircraft, medium haul 50-150 passenger aircraft, short haul 30-60 passenger aircraft and long haul major air carriers. The high lift needs for each type were found to be different, especially in emphasis.

The economic factors are initial cost, direct operating cost, total cost per seat mile, productivity in seat miles per hour per dollar, utilization potential in revenue miles per day, break even load factor and the particular market being addressed. Implicit herein is the extremely powerful factor of ever increasing prices of petroleum fuels for which in the foreseeable future there is no alternative.

The typical flight profile may be divided into several essentially independent segments with respect to the aircraft's high lift configurations: take-off ground roll, take-off climb to clear an obstacle, second segment take-off climb with one engine inoperative, clean climb to cruising altitude, cruising flight, descent, landing approach and touchdown, landing ground roll and alternatively, climb following an aborted landing. Each of the foregoing, under some circumstances, can be a limiting condition with respect to aircraft utility depending on factors such as field length, altitude, temperature, aircraft design characteristics such as power to weight ratio and the wing design, and, not the least, the constraining influence of Federal Aviation Regulations for insuring safe flight.

Aircraft lift and drag are proportional to the wing size and the airspeed squared. The constants of proportionality for lift and drag are C_L and C_D, varying with the angular attitude of the flight. Maximum lift at $C_L max$ would provide the lowest landing or take-off speeds and distances. Climbing performance is most strongly related to the lift to drag ratio L/D. Best range is obtained when the product of the speed times the lift to drag ratio is a maximum $(VxL/d)max$ (for jets). Sophisticated aircraft designs may provide a different high lift configuration for each segment of flight.

Pay-off potentials for a five per cent improvement in high lift for a flight segment limited jet transport can typically be a twenty per cent increase in payload at take-off, a forty-five per cent increase in useful load in second segment climb and a fifty per cent increase in payload when landing weight limited. Spectacular! However, it was found that whereas most aircraft specifications/designs call for maximal high lift capabilities, most aircraft operations are not constrained by high lift limitations. It would appear that if all existing aircraft were to suffer a five per cent reduction in their high lift capabilities the economic impact might go almost unnoticed. What then is driving high lift research and development? Among other factors aircraft are being inefficiently used on short hauls for which their configurations are not appropriate and the airlines are losing money, but deregulation will result in demands for the service being met by technologically and economically appropriate new aircraft.

Low initial cost, energy efficiency and user acceptance appear to be the most reliable measures of value. Higher lift at cruise speeds permits smaller, lighter cheaper wings if landing and take-off speeds and rates of climb can be met. Most of the new aircraft still on the sketch pads will have smaller more slender and straighter wings demanding all the increased high lift performance that can be obtained. The figure on the next page shows a plan view comparison of the potential dramatic reduction in wing size for a 30 passenger transport with advanced high lift.

Some pay-offs predicted for new aircraft applications of the best of today's state of the high lift art are:

High Speed Single Engine - 50% increases in cruise speed and range if $C_{Lmax} = 3.0$.

Short Haul Transport (see figure below)
-- 18% lower price
-- 24% less operating cost
-- 31% less fuel

Energy Efficient Transport
-- 18% less drag ($C_{Lmax} = 3.0$, could use 5.0)
-- 10% less fuel

While very large improvements are obtainable with today's best high lift technology, much more can be expected. The traditional two dimensional approach to high lift development should soon give way to full three-dimensional viscous flow high lift investigations made possible by the massive computer analysis and corresponding experimental data processing capabilities now in existence and being developed. Complete 3-D high lift optimization will, for example, result in a smooth spanwise blending of wing high lift devices,(flaps, modified leading edges, etc.) in contrast with today's all too typical usage of highly optimized two-dimensional airfoils chopped into extremely inefficient short spanwise segments having large lossy gaps between.

In summary, the rate of progress in high lift technology is high with improvements of 50% range over current operational use, economically attractive new families of aircraft have been identified in several thorough preliminary design study programs all of which show large benefits from improved high lift.

Two areas of possibly useful activity would seem to be:

1. Safe reductions of the presently required stall speed margins may be feasible through the development of better stalling behaviour.
2. "All Lifting" wing and tail combinations will require serious development because of the large potential gains in high lift.

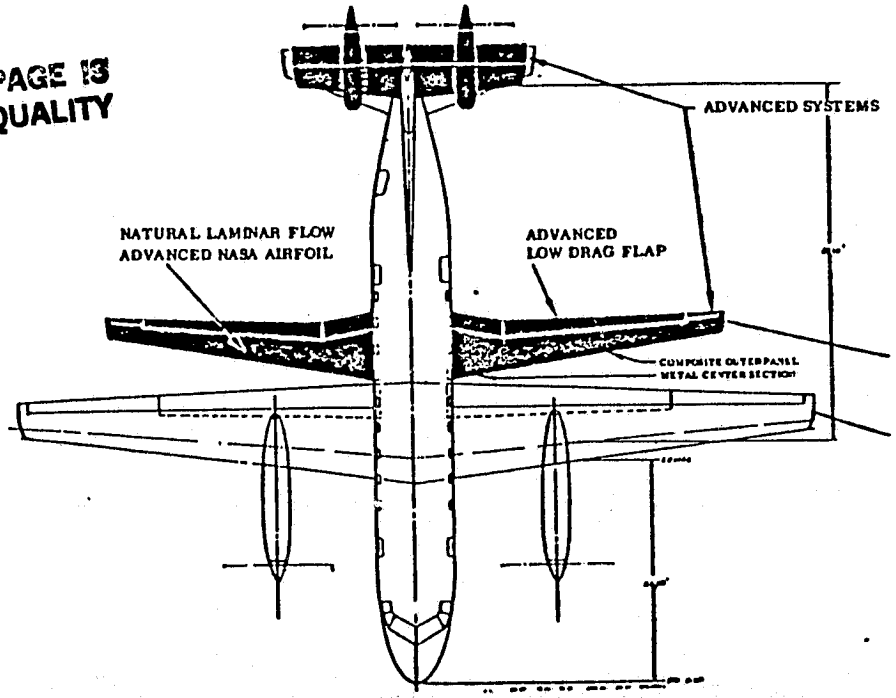

Computer Modeling Nucleotide Base and Base Pair Interactions with Amino Acids and Peptides

John S. Garavelli
Plant Sciences Department
Texas A & M University

This investigation was undertaken at the Extraterrestrial Research Division, NASA Ames Research Center, as a part of ongoing research into the origin and distribution of life and life-related chemistry in the universe. To achieve an explanation of the origin of the genetic apparatus of terrestrial life it will be necessary to understand the geometrics and energetics of the interactions between nucleic acids and proteins. Nucleic acids must rely on protein enzymes to replicate, and in order to synthesize proteins, nucleic acids must be transcribed and translated by molecular complexes consisting of both nucleic acid and protein components. The origin of such an intimately interconnected genetic apparatus may be explained through the study of the evolution of hypercyclic systems [1] but such an explanation will require a more complete description of the chemistry of the interacting components than is currently available.

An additional reason for undertaking this study is that recent advances in biotechnology have been absolutely dependent on the still fragmentary knowledge of the genetic apparatus and a more detailed understanding of the structure and mechanisms of this apparatus will be crucial for further advances. Some of the processes which have begun to be commercially exploited and which involve the interaction of nucleic acids and proteins are DNA replication, DNA packaging, RNA transcription, RNA processing, tRNA charging, and protein synthesis.

This research project consists entirely of computer model simulations of interacting nucleic acid and protein components which are created, manipulated and analyzed with AIMS, the Ames Interactive Molecular Modelling System. The work has progressed in five phases. The first phase consisted of correcting and reanalyzing the molecular structure data base. The available libraries of molecular models included nucleotide bases and amino acid side chains but these models contained systematic errors which were detected when preliminary energy calculations produced inconsistent results. The molecular geometries of these models were corrected to conform with the work of Arnott and Hukins [2,3] and to maintain a uniform set of hydrogen atom bonding distances [4]. Partial charge distributions for molecules with corrected geometries were reassigned with a program which calculated molecular orbitals using the MO-CNDO (Molecular Orbital by Complete Neglect of Differential Overlap) approach [5].

The second phase of the project consisted of developing a procedure for constructing hydrogen bonded molecular assemblies from the corrected molecular models. The procedure which was adopted employs the addition of phantom atoms at optimal hydrogen bonding distances and directions from potential hydrogen donating groups. One, two or three hydrogen bonds can then be formed between two molecules by superimposing the desired phantom atoms of one molecule on hydrogen accepting atoms of another molecule using a series of routines available in the MOLECULE program of AIMS. Two, one or no degrees of freedom, respectively, remain to be determined either by assignment or by minimization of non-bonded interaction energies.

In the third phase a library of hydrogen bonded molecular assemblies was produced. The molecular assemblies consist of either amino acid side chains or short segments of polypeptide backbone which are hydrogen bonded to either single nucleotide bases or base pairs already hydrogen bonded in the Watson-Crick scheme [6].

The intermolecular energy of each of these molecular assemblies was calculated in the fourth phase of the project. This was done with a routine available in MOLECULE which calculated the separate energy contributions of electrostatic, non-bonded, hydrogen bonded and torsional interactions empirically derived by Scheraga [7]. At this point it became evident that some of the assumptions about the various energy contributions might be unrealistic and that more work would be necessary to delineate clearly which potential energy terms must be improved and which terms might be neglected.

A fifth phase of the project involved initiation of the development of a routine to display graphically the results of intra- and intermolecular energy calculations. This routine which produces a plot similar to those introduced by Ramachandran [8] will be incorporated into the MOLECULE program. The table of energy values produced by this routine can also be used in information theory calculations of the apparent restricted conformation range of flexible molecules and molecular assemblies [9].

References

1. M. Eigen and P. Schuster, The Hypercycle: A Principle of Natural Self-Organization, (Springer-Verlag, New York, NY, 1979).

2. S. Arnott and D. W. L. Hukins, Biochemical and Biophysical Research Communications 47, 1504-1509 (1972).

3. S. Arnott and D. W. L. Hukins, Biochemical and Biophysical Research Communications 48, 1392-1399 (1972).

4. International Tables for X-ray Crystallography as cited in CRC Handbook of Chemistry and Physics, 53rd edition (CRC Press, Cleveland, OH, 1972), p. F-179.

5. J. A. Pople and D. L. Beveridge, Approximate Molecular Orbital Theory (McGraw-Hill, New York, NY, 1970).

6. J. D. Watson and F. H. Crick, Nature (London) 171, 737 (1953).

7. H. A. Scheraga, et al., Quantum Chemistry Program Exchange, Program No. 286 (Chemistry Department, Indiana University, Bloomington, IN, 1975).

8. G. N. Ramachandran and V. Sasisekhoran, Advances in Protein Chemistry 23, 283 (1968).

9. J. S. Garavelli, I. Studies on the Structure of Mitochondrial Malate Dehydrogenase II. Applications of Information Theory to Protein Structure (Ph.D. dissertation, Biochemistry Department, Washington University, Saint Louis, MO, 1975).

NASA/ASEE SUMMER FELLOWSHIP REPORT
PACER INSTRUMENTATION SYSTEM

Prepared 23-AUG-82 by

Arthur W. Hoadley
Assoc. Prof. Western Michigan Univ.

The Pacer Instrumentations system, when completed, will display precise values of mach number, altitude, and airspeed to the pilot and/or flight test engineer while pacing an aircraft undergoing flight testing. Present requirements call for the first unit to be installed in an F-104 airplane. The system will give the operator the ability to freeze the display for close observation and to select corrected or uncorrected display data.

The hardware will consist of a two board computer system. One of the boards presently under design at NASA holds the microprocessor (CPU), arithmetic processer (APU), volatile and non volatile memory, and serial and parallel input/output (I/O) ports. The remaining board in the Pacer system will interface with two Garrett pressure transducers and the display unit. Provisions will also be made to interface with a flight data recorder and/or a printer. The display under present consideration is a liquid crystal display consisting of two lines of forty characters each.

Throughout the entire design, the broader applications of the hardware and software have been of high priority. The main system board contains the power and flexibility necessary in almost all the on board computer applications. The display unit promises to be a very flexible means of presenting information in a host of projects. For these reasons, the software written to drive the display, I/O ports, and the arithmetic processor has been written as a set of upper level commands to be used by an assembly language programmer.

To date the hardware and software have been developing simultaneously. The main thrust of this fellowship has been the development of the software necessary to utilize the arithmetic processor and drive the display. The result of this work has been the creation of a set of macros and subroutines that may be called from an assembly language program to perform math functions similar to those found on a scientific calculator. A manual entitled 'APU (8231) FUNCTIONS MANUAL,13-Aug-82 A.W. Hoadley' has been prepared documenting the software written specifically for the APU and the CPU being used on the main system board. (the table of contents of this manual is included in the appendix.) The programs can be used with no further modifications using the 8085 cross assembler on the PDP 11/34. Included also in this document is an example applications program (PACER4.SRC), which is the program written to perform the calculations required by the Pacer project.

The Pacer program starts with two 20 bit input data words from the pressure transducers representing the measured total and static pressures. The calibrations are then applied to the inputs using a polynomial solution. This solution is accomplished by calling the POLY, function written for the APU. Next the pressure ratio is calculated using the DIV, function to perform the division. As the program continues the mach number is corrected using the table lookup and interpolation function (LOKUP,). This function looks up a specific independent variable value in a table and returns to the user the correct interpolated value of the dependent variable. The

calculations continue in this manner until the values of mach number, altitude, and airspeed are calculated. These values are then converted to ASCII format using the CONVER function and then displayed.

As described above the PACER6.SRC program makes extensive use of the macros and subroutines written for the APU and CPU. These functions can easily be used to solve necessary equations required by future projects using the APU and CPU thus giving this work many future applications.

Each function in the manual is described in the following format:

NAME:

LOKUP, OP1,OP2,OP3,OP4,OP5,OP6,OP7

SYNOPSIS:

The table lookup function will search a given table to find the closest values to the given independent variable. Linear interpolation is then used to find the desired result.

DESCRIPTION:

The operands are defined as follows:

OP1 = address of independent variable to be found in table
OP2 = address of first independent variable value in table
OP3 = address of first dependent variable value in table
OP4 = the number of values of the independent variables provided in the table
OP5 = the address of a scratch memory area (16 bytes)
OP6 = address where the program will jump if the number stored at address OP1 is outside of the values provided in the table.
OP7 = the address where the result will be stored

Before using the LOKUP, function the user must establish the table of values using the following format.

```
OP4:   EQU    xxH
OP2:   DW     xxxxH,yyyyH     (see ENTER.)
       |
       |
OP3:   DW     xxxxH,yyyyH     (see ENTER.)
       |
       |
```

NOTE: The above groups of data need to be in ascending order.

RESULTS:

The results are stored at address OP7.

APPENDIX

APU (8132) FUNCTIONS MANUAL

TABLE OF CONTENTS

Measuring Pilot Workload in a Moving-Base Simulator

Barry H. Kantowitz

Purdue University
Professor of Psychological Sciences and Industrial Engineering

There are three major techniques for measuring pilot workload: subjective meaurement, objective measurement, and physiological measurement. The greatest success has been obtained with subjective ratings where pilots are asked to complete assorted rating scales after a flight. However, there is no rigorous theoretical framework to explain what such ratings mean, except perhaps for mathematical scaling models that contain no axioms related to the content area of workload evaluation. Since it is well-known that pilots (and other humans) cannot provide introspective reports with complete accuracy, it is essential to validate these rating data with objective procedures. So far, researchers have not been able to obtain systematic workload effects based upon objective measures of behavior.

I believe that substantial advances in human factors will come about only when theory from basic research is combined with practical problems (Kantowitz, 1981). Objective measurement of pilot workload is a sufficiently difficult and challenging problem to serve as a test bed for application of theory to a practical problem where most investigators have been unable to find good answers. I came to NASA-Ames this summer to (1)put my money where my mouth is and try to solve an important practical problem by approaching it from a theoretical perspective, and (2) get my hands on a GAT flight simulator, a piece of equipment not available to me at Purdue.

Despite the valiant efforts of my NASA colleague Sandra Hart who had been sending in work orders since last Februrary, the GAT simulator was not flying when I arrived at the beginning of the summer. Once the GAT was flying properly, we discovered that the signal conditioner used to record analog data from the GAT needed work. Making the necessary repairs, checking calibration, and adding a four-position switch to the GAT yoke consumed almost five weeks. I used two of these weeks to write a computer program to control and record the secondary reaction-time task I would use as an objective measure of workload since the programmer assigned to the project had quit leaving the group temporarily without a professional programmer. Another week was spent writing a complex data analysis program. By now I was almost as good a programmer as I was during my graduate student days. To further polish my dormmant programming skills I sat in on EE 611, televised at Ames; this was most useful and an unanticipated bonus of my summer. I am grateful to the co-ordinators for informing me of this televised course.

At long last the day of reckoning arrived: We tested our first experimental subject. The reaction time data were exactly what the theory predicted. Alas, the GAT signal conditioner became unplugged during the experiment and so these data had to be discarded because it is essential to record both primary and secondary task performance. As of this writing, the experiment is in full swing and data collection will be completed the day I leave (if all subjects show up as scheduled and the equipment keeps on running). Tentative results (see figure) give grounds for cautious optimism. It appears possible to provide an objective measure of pilot workload. However, firm conclusions need await the complete data analyses

:o be performed at Purdue. Additional work, such as expanding the GAT flight scenarios and analyzing the micro-structure and instantaneous workload, could be done next summer.

Experimental research with human subjects is always frustrating, and .n this regard despite its superior equipment and technical support facilities, Ames is very much like a university. Things always take longer than you plan. Although the chance to use special equipment was what brought me to Ames, there were many other benefits gained. Discussions with Sandra Hart and members of her group taught me a great deal about aviation and the problems pilots face. Professors Dan Weintraub and Earl Weiner were visting Ames and we had many helpful conversations about my project. The Wednesday evening lectures were uniformly of high quality; this was the first time in years that I have paid attention to events outside my own discipline and the effort was well worth it. When I return to Purdue I shall try harder to attend lectures outside psychology and industrial engineering. All in all, the summer was challenging and exciting. It allowed me to discover a new area with interesting problems that are related to my own theoretical interests in human attention and information processing.

Reference

Kantowitz, B.H. Interfacing engineering psychology and human information processing. In W. Howell & E. Fleishman (Eds.), Human performance and productivity, Vol. 2. Hillsdale, N.J.: Lawrence Erlbaum Associates, 1981.

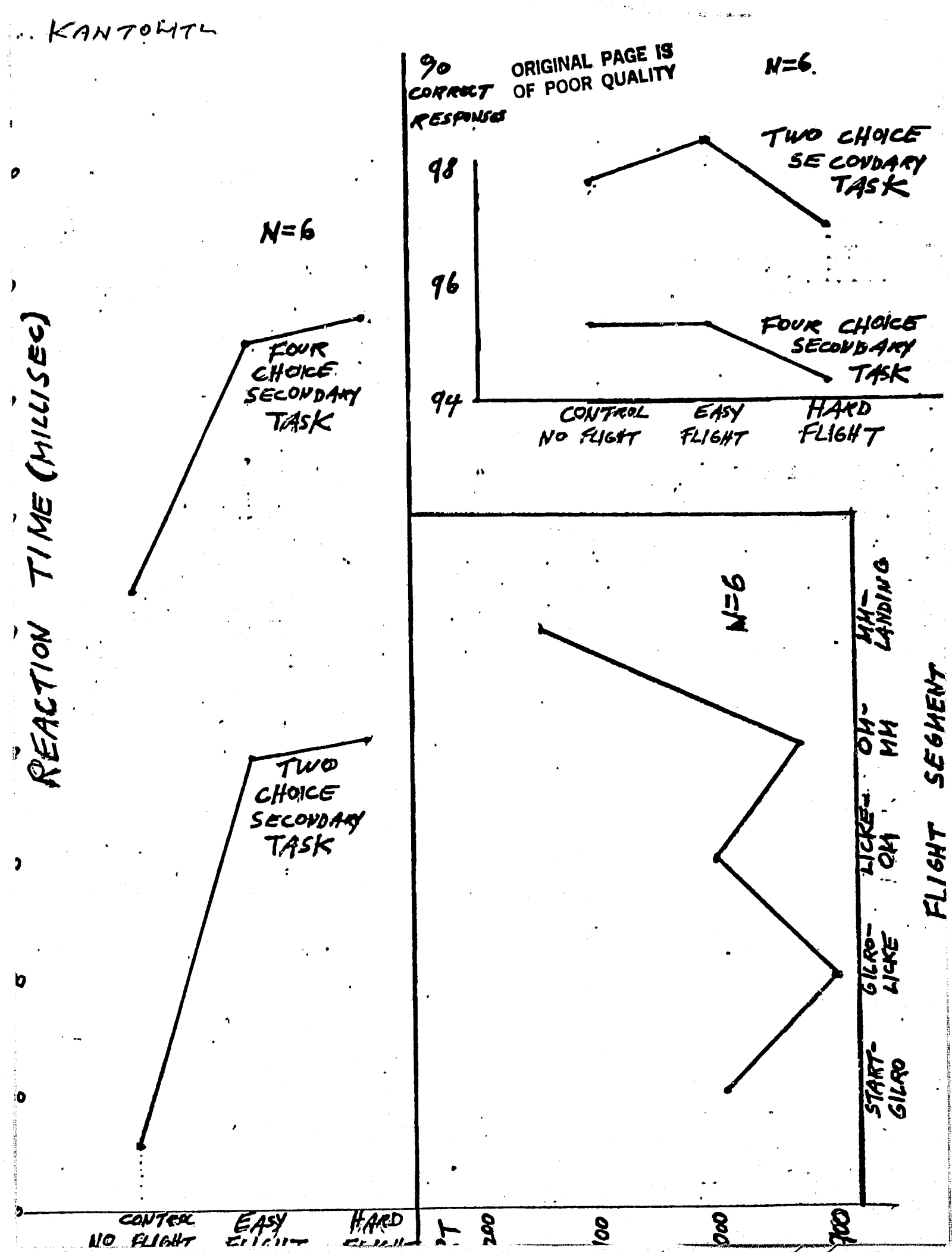

Implicit Model Following as applied to the Forward Swept Wing.

David Kozel

Purdue University Calumet
Assistant Professor of Engineering

The purpose of the project I worked on this summer was to repeat the work done by Grumman on the control law design of the Forward Swept Wing.

The Forward Swept Wing is a control configured vehicle, which has some unstable modes. For this reason, a proper and robust controller is essential. Grumman used the method of discrete implicit model following to produce their gains for the control laws. Also, they added an integrator in the forward loop to make the system type one. An algorithm was then used on the gains so that the output of the forward loop integrator, an unobservable state, was not fed back.

The first step of the project was to develope the command augmented state equations (in general form) for, the model to be followed and the aircraft. This was done for the longitudinal up and away mode. The model state equations were derived from a transfer function of the model taken from a technical report published by Grumman.[1] The aircraft state equations were derived partially from the output of a linearization program developed by Joseph Gera of NASA, Dryden, and partially from augmenting on terms representing actuators and a forward loop integrator. Afterwards, both sets of equations were augmented by an equation representing the form of the pilot input. Since the controller was for a digital fly by wire system, the equations were then discretized.

The second step of the project was to develop an algorithm to solve the discrete implicit model following problem.[2] This was done by transforming the discrete implicit model following problem to the discrete linear regulator problem without cross product terms in the performance index; which was done by using two transformations. Then, the steady state solution to the discrete linear regulator problem was obtained using an algorithm developed by Vaughan.[3] The result was improved using the oracles routines. Then, transforming back the results, the discrete control law gains were obtained.

The third step of the project was to develop an algorithm that would take the gains resulting from the solution of the discrete implicit model following problem. Gains that included the output of the forward loop integrator. To gains that did not include the output of the forward loop integrator, but did include the values of the other states

at that time instant and the previous one. A similiar algorithm for the continuous case was developed by Anderson and Moore.[4]

The fourth step of the project was to write a program that given the augmented state equations for the model and aircraft, the relationship between the two sets of states, and the desired performance index, it would descretize the system, solve the discrete implicit model following problem, and transform the resulting gains as mentioned above.

The following still needs to be completed: Derivation of the augmented model and airgraft state equations and their resulting control laws, for the other modes of the aircraft; Investigation of the capabilities and limitations of discrete implicit model following as a design methodology. Both of which can be very much aided by the program developed this summer.

References

1. Spacht, G. and Calandra, J., 1980, Forward Swept Wing Demonstrator Technology Integration and Evaluation Study, Volume 1, Report Number AFWAL-TR-80-3145

2. Gran R. and Berman H., "Optimal Digital Flight Control for Fighter Aircraft" Journal of Aircraft, Jan. 1977, p. 32-37.

3. Vaughan, D. "A Nonrecursive Algebraic Solution for the Discrete Riccati Equation", IEEE Transactions on Automatic Control, Oct. 1969, p. 598-600

4. Anderson, B. and Moore, J., Linear Optimal Control, Prentice Hall, Englewood Cliffs, N.J., 1971.

5. Armstrong, E., ORACLS- A System for Linear-Quadratic-Gaussian Control Law Design, NASA Technical Paper 1106, April 1978

A Study of Rat Bone Cells

Summer Research in Life Sciences Division at NASA-Ames Research Center.

June 21, August 27, 1982

P. Wesley Lawless, Fordham University

Dr. Adrian Mandel, NASA-Ames Coordinator

The project began in conference with Dr. Mandel and Ms. JoAnn Williams. A computer literature search (Medlars at SUNY) by the life sciences research librarian gave 56 pertinent abstracts. The key words were: rat, hybridoma, monoclonal antibodies, calvaria, osteoblasts, osteoclasts.

The study resolved into three phases: (a) production of hybridomas to yield mouse monoclonal antibodies against rat bone cells; (b) separation of the bone cells into subpopulations; (c) isolation and characterization of cellular antigens from the subpopulations.

I. Monoclonal Antibodies

Three clones were sought: (a) against bone cells, (b) against a glycoprotein surface antigen which binds to both Con-A and Lentil lection, (c) against a glycoprotein which binds to Peanut Lectin and Soybean Lectin. The procedure followed that of Kohler and Milstein. (1)

Three BALB/c mice were injected i.p. with 1×10^7 bone cells. The bone cells had previously been prepared from neonatal rat calvaria by Ms JoAnn Williams and Dr. Emily Holton. Three mice were injected i.p. with the Con-A and Lentil glycoprotein and three with the Peanut and Soybean glycoprotein. In the latter two cases, 100 ug in 100 ul were injected followed in ten days by 10 ug boost.

Four days after the last injections the mice were sacrificed. Their sera were saved and tested for the antibodies. Antibodies were present in the three experiments.

The mice spleens were removed; splenocytes separated between frosted slides, washed and suspended in serum-free RPMI medium. Cells from a mouse myeloma line, SP2/o were also suspended in serum-free RPMI. Equal numbers of splenocytes and myeloma cells were mixed and pelleted together at 200g x 10 min. The supernatant was discarded.

One ml of 50% PEG (polyethylene glycol) was added to the pelleted cells for one minute at 37°C immediately followed by the addition of 1 ml of serum-free RPMI for one minute. Another ml was added for a minute followed by seven milliliters. The cells were gently pelleted and resuspended in 30 ml of complete medium (RPMP, fetal calf serum, penicillin-streptomycin, glutamate, pyruvate). This volume was aliquoted into 3-96well microtiter plates and incubated overnight at 37°C, 10% CO_2, humidified atmosphere. The following morning, the mddium was changed to HAT medium (hypoxanthine-aminopterin-thymidine). In this medium, fusions of myeloma-splenocytes will grow but not myeloma-myeloma or splenocyte-splenocyte. Half of the volume of the medium was removed and replaced by an equal volume of HAT on days 1,2,3,5,8, 11. Then the medium was changed to HT complete medium. After a week the wells were assayed for antibody production. The positive well contents were transferred to 24 well, 1 ml plates to which had been added feeder thymocytes.

The cells in the 24-well plates were selectively diluted in order to isolate cells which could be cloned giving the desired antibodies.

ELISA (enzyme-linked immunosorbent assay) (2)

We preferred this technique to RIA as our assay for antibody because it is less expensive and less hazardous. 96 well microtiter plates were coated with either cells or protein. Cells were added to wells first treated with poly-lysine. They were then fixed with 0.5% gluteraldehyde and washed with 0.1 N Glycine. Protein was added at 10 ug/ml in 0.1 $NaHCO_3$, pH 9.6 and incubated 2 hr, 37°C. Supernatants from the wells of the fused cells were added to the coated wells and incubated at room temperature for four hours. The plates were washed in 0.1% detergent and goat anti-mouse antibody conjugated with alkaline-phosphatase was added overnight at room temperature. In the morning the plates were washed and filled with substrate, PNPP, p-nitrophenyl phosphate(colorless). If the enzyme was present, the substrate changed yellow (p-nitrophenol). Colored wells were considered positive indicating that the supernatants contained the antibody to cells or protein.

II. Surface Antigens

Bone cells, 1×10^7, were solubilized in 2 ml 0.5% NP-40 (nonidet) for 10 minutes, 4°C. The tubes were centrifuged 20 min, 3000 rpm and any insoluble material discarded. The contents were dialyzed against PBS (phosphate buffered saline) to remove the detergent. The dialysate was passed through a 1 ml Peanut-agarose (1mg/1 ml agarose) column which was washed with PBS. When no further protein was eluted as determined by absorbancy at 280 nm, the column was eluted with 0.2 M galactose followed by 0.1 M borate. Protein was eluted and was labelled Galactose-plus glycoprotein. The experiment was repeated using Soybean lectin-agarose and the same glycoprotein was obtained.

The solution eluted with PBS wash from the above columns was passed through 1 ml columns of Con-A agarose and Lentil-agarose. Each column was washed extensively with PBS and eluted with 0.2 glucose followed by 0.1 borate and 0.2 sucrose. These elutions were pooled and dialyzed and protein concentrations determined. They were labeled glucose-plus glycoprotein.

The galactose(+) and glucose (+) compounds were passed through Sephadex G-200, 30 ml columns and eluted with PBS. One peak came through for galactose (+). A major peak came through for the glucose (+) compound and a lesser peak which was a multiple of the molecular weight for the larger one.

The proteins were further studied on SDS-PAGE (polyacrylamide gel electrophoresis). Purities were found to be singular and their molecular weights determined which were the same estimated from G-200.

III. Subpopulations of Bone Cells (3)

A fifteen milliliter solution of 20% fetal calf serum, heat denatured at 56° 30 min, and PBS was prepared. Bone cells were mixed with peanut lectin and layered on this column. A buffy layer formed at the top. After 30 min in the cold, some cells had sunk to the bottom; most had remained in the buffy layer. The cells at the bottom were removed and suspended in 10 ml of 0.2 galactose in cold for 10 min. They were pelleted by spinning at 200g x 10 min. These cells were labelled Galactose(+) cells.

This experiment was repeated using lentil lectin. Again cells sank to the bottom of the FCS-PBS column after 30 min in cold. These were suspended in 10 ml 0.2 M glucose and centifuged. They were labelled glucose (+) cells.

We are currently comparing histochemically the three cell populations: glucose (+), galactose (+), and glucose-galactose (-).

We have used our two glycoproteins to immunize mice and are developing hybridomas to yield specific monoclonal antibodies.

We wish to thank Dr. Adrian Mandel and Ms JoAnn Williams for their cooperation and helps and the administrators of the NASA-ASEE Stanford University program for permitting me to be a part of this project.

References:

1. Monoclonal Antibodies. eds. Roger H. Kennett, Thomas J. McKearn, Kathleen Bechtol, Plenum Press, N.Y., 1981.

Selected Methods in Cellular Immunology, Barbara B. Mishell and Stanley M. Shiigi, W.H. Freeman, San Francisco, 1980.

Kohler, G. and Milstein, C., Eur. J. Immunol. 6, 511-519, 1976.

2. Engvall, E. and Perlmann, P., Immunochemistry, 8: 871, 1971.

3. Pearlstein, E., Exp. Cell Res., 109, 95-103, 1977.

Reisner, Yair, and Nathan Sharon, TIBS, 29-31, 1980.

The Application of Aerostatic Thrust Bearings in Minimizing External Noise Generation on the NASA Ames Vestibular Research Facility

Robert Lincoln

California Polytechnic State University
Lecturer, Aeronautical/Mechanical Engineering Department

In NASA's space motion sickness research meaningful and valid scientific measurements must be taken of the inner ear's vestibular system. It is imperative that external noise or vibrations on the test equipment be kept to a minimum. Scientific study done on various specimens' vestibular systems concludes that external vibrations in the vertical direction must be kept below 500 μg's (5×10^{-4} times gravitational acceleration) between frequencies of zero to 100 cycles per second. Preliminary study on a linear accelerator track apparatus indicated that an unconventional bearing system would be necessary to keep vibrations below the 500 μg level. Therefore, the suitability of air bearings became a necessary research area.

Air bearings fall into two primary classifications: fixed orifice and porous. Vibration measurements were taken on three commercially available air bearings and in addition to these a series of measurements was taken on a roller bearing supported system built and operated by M.I.T. As expected the roller bearings gave vertical accelerations far in excess of the 500 μg level. The maximum acceleration had a magnitude of 3.6 mg(3600 μg) at 22Hz. Hard bearings proved to be definitely unsuitable for our purposes but interesting for comparison purposes.

The first of the air bearing systems tested was one in use here at NASA Ames. A 3-axis coordinate measuring machine built by Brown & Sharpe Mfg. Co. uses air bearings to hover between 0.0003 and 0.0006 inches above a granite slab. This particular bearing had both single and multiple discrete orifice arrangements with a system of grooves which distributed the air flow over the bearing interface. A plot of acceleration as a function of frequency was obtained by doing a Fourier analysis with data from Sundstrand accelerometers. Although this bearing produced audible noise, the vibration magnitudes measured in the dynamic mode were acceptable as the maximum acceleration was 340 μg at 25 Hz.

A porous type thrust bearing system found on a coordinate measuring machine built by Bendix Corp. was the next type tested. As its name implies, a porous bearing consists of a perforated surface resulting from a large number of tiny orifices, typically 0.1 mm in diameter. This bearing produced no audible noise and gave vibration levels well below that of the Brown & Sharpe version. The

peak acceleration was 125 μg at 20 Hz. An interesting note to the tests run on this system is that some damping occurred in the dynamic mode as the accelerations it produced were smaller in magnitude than in the static mode.

The final system tested proved to be the most impressive and promising. A custom air bearing shop, Fox International Inc. allowed us to test a carriage/monorail setup designed for laser applications. The carriage was supported by eight circular discrete orifice bearings: 4 on the sled bottom and two on each side. This particular design had three orifices spaced 120° apart that fed into a channel system. After two dynamic runs the maximum acceleration was 62 μg at 55 Hz (shown on pg. 3). Therefore, this discrete orifice, minimum film thickness bearing has a maximum vertical acceleration half that of the porous type tested. This bearing or a similar version of Fox International's appears to be more than satisfactory for our use on the Vestibular Research Facility linear accelerator.

References

1. Powell, Grassom, 1964, Gas Lubricated Bearings, Ch.1,4, pp. 158-161

2. Duckworth, R.A., 1971, Gas Bearing Symposium #18, "An Experimental Study of Externally Pressurized Steam-Lubricated Bearings."

Fox International, Inc. 8/10/82
12:32PM

| FAST MOVING |
30 psi
40# WT

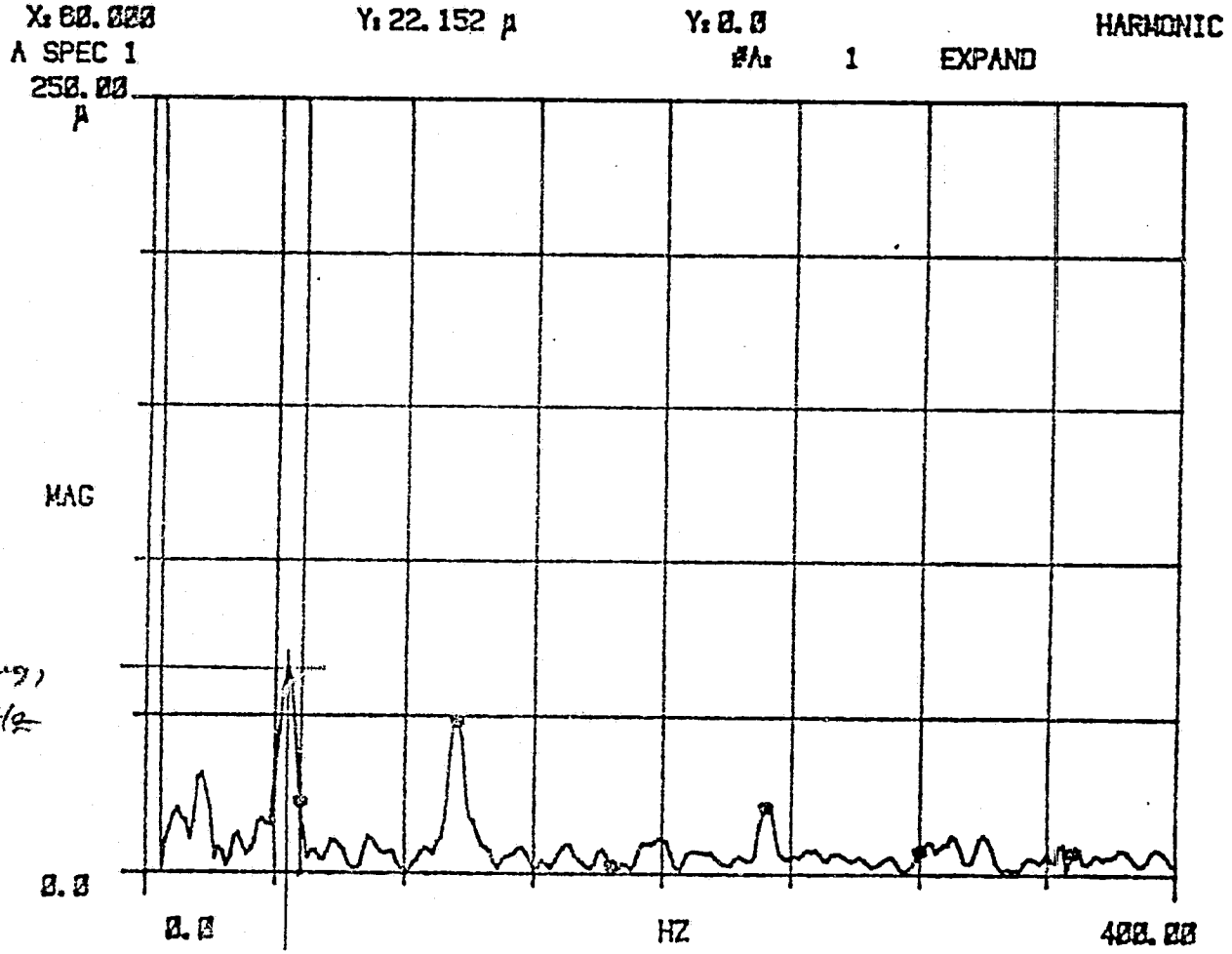

ASEE SUMMER RESEARCH REPORT

DAVID J. NOLTING

1982

My work this summer involved the study of absolute stability regions of linear multistep formulas in the solution of the ordinary differential equation

$$dy/dx = f[x,y]. \qquad [1]$$

My specific aim was to search for explicit linear multistep formulas having absolute stability regions that included larger portions of the imaginary axis about zero than those regions of previously known explicit formulas. I conducted the search within the order-classes of formulas for which the order is the same as the number of backpoints. Starting at the lower orders, I completed the investigation through order three and have the program prepared for the fourth order search. The Euler explicit formula is the only member of the class of order one. I will discuss the results for orders two and three.

The second order class of such explicit formulas have only one free parameter. If we choose that free parameter to be the coefficient of the backmost y-value [call it a1], then these formulas can be represented as follows when applied to equation [1]. [subscripts are given in parentheses]

$$y(n+1) = [1-a1]*y(n) + a1*y(n-1) + .5*h*([3+a1]*f(n) + [-1+a1]*f(n-1)) \qquad [2]$$

The values of a1 which allow stability at $h=0$ are those for which $-1 < a1 < 1$. The stability regions collapse from the circle $z = e^{i\theta} - 1$ when $a1 = -1$, to the line segment on the imaginary axis between i and -i, when $a1 = 1$. This is sketched in the sequence of illustrations shown below in the $h\lambda$-plane.

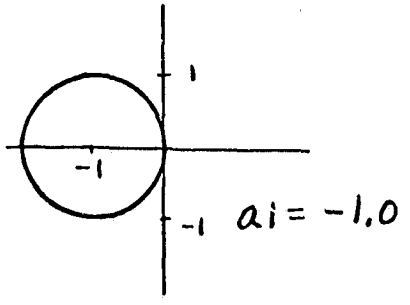

a1 = -1.0

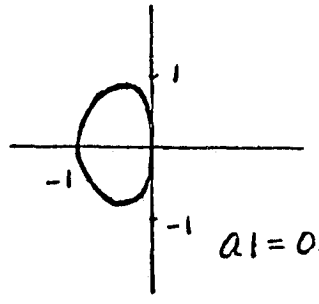

a1 = 0.0

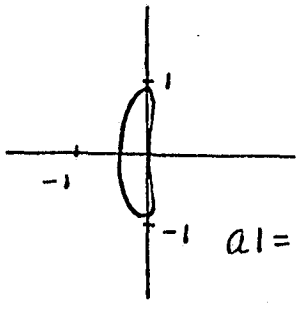

a1 = 0.67

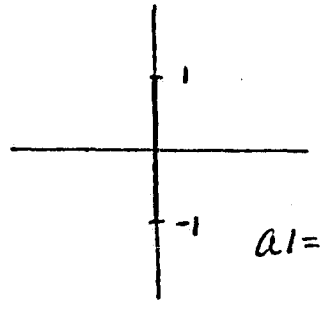

a1 = 1.0

The third order class of formulas has two free parameters. When these two parameters are taken to be the coefficients of the two backmost y-values [say a1 and a2], then this class of formulas can be represented as follows.

$$y(n+1) = [1-a1-a2]*y(n) + a1*y(n-1) + a2*y(n-2) + [1/12]*h*[[23+5*a1+4*a2]*f(n) + [-16+8*a1+16*a2]*f(n-1) + [5-a1+4*a2]*f(n-2)] \quad [3]$$

The values of a1 and a2 which provide stability at h = 0 are those which satisfy the following system of linear inequalities.

$$\begin{aligned} 1 - a1 &> 0 \\ 1 - a2 &> 0 \\ 1 + a1 + 2*a2 &> 0 \end{aligned} \quad [4]$$

The stability regions vary throughout this feasible region, however, in regard to the measurement of stability on the imaginary axis, they are little better than the second order methods discussed previously. In fact the familiar third order Adams-Bashforth formula [a1 = a2 = 0] is very competitive. Typical stability regions for members of this class are given below.

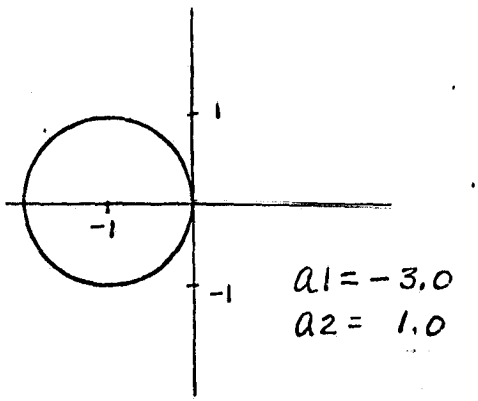

a1 = -3.0
a2 = 1.0

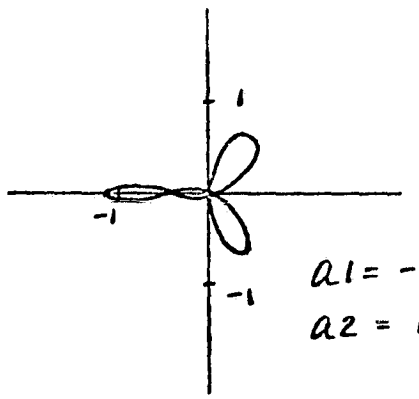

a1 = -1.0
a2 = 1.0

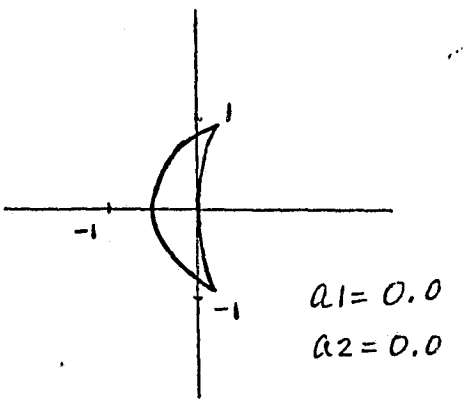

a1 = 0.0
a2 = 0.0

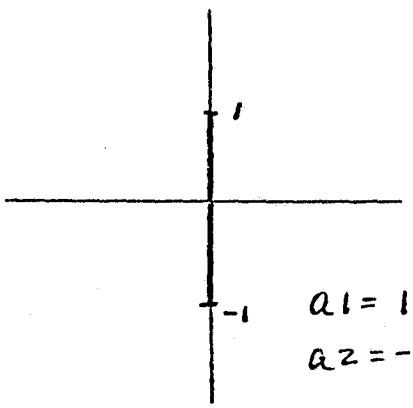

a1 = 1.0
a2 = -1.0

As mentioned earlier, the programming is ready for the fourth order investigation, however, time did not permit its completion. A couple of other interesting points were noted during the summer's work. I will state the first as a conjecture.

Conjecture: Let L be an explicit linear k-step, kth-order formula of the form

$$y(n+1) = y(n-k-1) + h*\sum_{i=0}^{k-1} b(i)*f(n-i),$$

where k is even. Then the absolute stability region of L is an interval about zero on the imaginary axis.

Numerical results for k = 1, 2, 3, and 4 have been consistent with this conjecture. In addition, a sketch of a proof has also been supportive. I did not take the time to pursue a careful proof, although the direction to pursue is evident. This type stability region exists for a third order formula also as we noted in the sketches following the previous paragraph. I did not attempt a generalization for odd-ordered formulas.

The second point of interest follows from a consideration of the absolute stability region for the scheme defined by the pair of equations below.***

$$Y(n+1) = [1 + z]*y(n)$$

$$y(n+1) = [1 + g*z]*Y(n+1) \qquad [5]$$

In these equations z is the eigenvalue-stepsize product, and g is an arbitrary real parameter. The stability polynomial for the scheme above is

$$p[g,z] = 1 + [1+g]*z + g*z**2. \qquad [6]$$

The following result is established.

Theorem: The closure of the absolute stability region of the scheme [5] contains the boundary of the absolute stability region of Euler's explicit formula for $\emptyset < g < 1$.

Proof: The absolute stability boundary of Euler's explicit formula is $z = e^{i\theta} - 1$. Consider $p[g,e^{i\theta} - 1]$, where p is taken from [6]. The magnitude of $p[g,e^{i\theta} - 1]$ is the magnitude of the quantity

$$g*e^{i\theta} + 1 - g. \qquad [7]$$

Of interest are those values of g for which [7] is contained in the closed unit disk. Since the unit disk, $g*e^{i\theta}$, and [7] are each circular with center on the real axis, we may reduce our concern to $\theta = \emptyset$, and π. When $\theta = \emptyset$, [7] reduces to 1 for all g. When $\theta = \pi$, [7] becomes 1 - 2*g which is in the closed unit disk for $\emptyset < g < 1$.

*** From oral communication with Harvard Lomax.

NONLINEAR SOLUTION TECHNIQUES FOR THE DISCRETIZED STEADY-STATE EULER EQUATIONS

Charles W.Schelin

The Euler equations amount to a system of conservation laws that may be used to describe inviscid fluid flow. Many numerical schemes have been developed to solve these equations using time step methods. If one is concerned only with the steady state solution the iterative steps toward this solution need not be time accurate. Thus it may be possible to obtain the steady-state solution more rapidly using nonlinear schemes whose iterative steps are in some sense independent of time.

Dennis Jespersen of NASA-Ames has successfully applied Newton's method to the steady-state Euler equations using a Gauss-Seidel multigrid scheme to solve the linear system for each Newton step. I began this summer's work trying to speed up his scheme.

After a few week's work,I was able to reduce the computing time required on some of the intermediate Newton steps by iterating only on those nodes where a sufficiently large change was indicated. Regular Newton steps were still necessary, however, at the beginning and to finally obtain a converged solution.

In the hope that a faster scheme could be developed I spent the remainder of the summer analyzing the nonlinear difference equations that arise when the steady state Euler equations are discretized using the flux-vector splitting of Steger and Warming [1] and the second order one-sided differences used by Jespersen. These equations are linear combinations of the generalized flux-split vectors E and F evaluated at grid point (i,j) and up to eight neighboring points. Letting d,u,v,c represent density, horizontal and vertical components of velocity, and local sound speed, respectively, one finds that the vectors

E = (e1,e2,e3,e4), and F=(f1,f2,f3,f4),

satisfy

```
e1 = d*(.8*w1 + w2)
e2 = u*e1 + d*c*w3
e3 = v*e1
e4 = u*e2 + v*e3 - .5*e1*(u**2 + v**2) + 2.5*w2*d*c**2

f1 = d*(.8*z1 + z2)
f2 = u*f1
f3 = v*f1 + d*c*z3
f4 = u*f2 + v*f3 -.5*f1*(u**2 + v**2) + 2.5*z2*d*c**2
```

where

```
w1 = (u +/-abs(u))/2
w2 =  u +/-(abs(u+c) + abs(u-c))/2
w3 =  c +/-(abs(u+c) - abs(u-c))/2
```

and z1,z2,z3 are obtained from w1,w2,w3 by replacing u with v. Using these properties, I considered a point Gauss-Seidel solution scheme.

A point Gauss-Seidel scheme amounts to solving for the variables d,u,v,c at point (i,j) using the latest values of these variables at neighboring points. Such a scheme thus requires solving a nonlinear system of the form

```
g1(d,u,v,c) = b1
g2(d,u,v,c) = b2
g3(d,u,v,c) = b3
g4(d,u,v,c) = b4
```

at each grid point. Taking T = d*c, if b1 > 0 and b4*b1 > .5*(b2**2 + b3**2), I have shown that this system has a solution. When u < c one finds

```
v = b3/(2*X'*T + b1)
u = b2/(2*Y'*T + b1)
c = .8*(Y'*abs(u) + X'*abs(v))*T/(b1 - 2*(X'+Y'))
```

where X' and Y' are derivatives of the coordinate transformation and T must satisfy g(T) = 0, where

```
g(T) = 5*(X'+Y')*T*c**2 - b4 + b3*v + b2*u - .5*(b2**2 + b3**2).
```

In the supersonic case the formulas for u and c are more complicated, specifically

```
u = (b1*b2**2-(1.6*X'*Y'*abs(b3)+4*b2*X'**2)*T**2)/h,
```

where

```
h = (2*X'*T+b1)*((5.6*Y'*T)**2-2*X'*b1*T+b1**2),
```

and

```
c = (b2-b1*u)/(2*Y'*T).
```

In this case, g(T) is altered by replacing 5*(X'+Y')*T*c**2 with 5*(X'*c+Y'*u)*T*c. If T' is selected so that u = c, and if g(T') < 0 then the system admits a unique solution T in the interval (T',R) where u < c and R = b1/(2*(X'+Y')). If g(T') > 0, the system has a solution in the interval (0,T') where u > c, but none with u > c.

I have written a FORTRAN code for this scheme which I am taking back with me to UW-LaCrosse for further refinement. Thanks to Dennis Jespersen and the other fine people at NASA-Ames this summer's experience has opened an exciting area of research to me. With continued work I hope to obtain results that are worthwhile computationally.

REFERENCES

1. Steger,J.L. and Warming,R.F.,Flux Vector Splitting of the Inviscid Gasdynamics Equations with Finite-Difference Methods,J.Comp.Physics,v.40,pp.263,293(1981).

Stability of the Flow past a Cylinder

Roger Schlafly

Dept. of Mathematics, University of Chicago

This project concerned the computer modelling of a viscous incompressible fluid flowing past a circular cylinder. The flow is assumed to have constant velocity at infinity. The problem reduces to that of a two-dimensional flow past a disk.

Properties of the flow are determined by the Reynolds' number, which is defined to be

$$R = \frac{u_\infty \cdot \ell}{\nu}$$

where u_∞ is the speed at infinity, ℓ is the diameter of the cylinder, and ν is the viscosity. The velocity vector of the flow satisfies the Navier-Stokes equations:

$$\frac{\partial u}{\partial t} + u \cdot \nabla u = \nu \nabla^2 u - \nabla p$$

$$\nabla \cdot u = 0$$

where p is the pressure. A computer program to solve these equations numerically has been developed by Unmeel B. Mehta of NASA-Ames [1]. A listing of his program may be found in [4].

There is a critical Reynolds' number R_0 such that for $R < R_0$, the flow eventually converges to a steady-state flow. The flow is stable, meaning that any small perturbation quickly dies away. When $R > R_0$, the flow becomes unsteady, with eddies constantly forming and being carried downstream. It has been experimentally determined [3] that $R_0 = 48 \pm 1$. The generally accepted explanation for this is through a bifurcation of the solution to the Navier-Stokes equations. There is, presumably, a steady-state solution for $R > R_0$ but it is unstable.

My project, suggested by Murray Tobak of NASA-Ames, was to obtain some numerical evidence for this explanation through computer simulations. The Navier-Stokes equations, written in terms of the vorticity ψ, are:

$$\frac{\partial}{\partial t}\nabla^2\psi = \nu\nabla^4\psi + \nabla\psi \times \nabla^3\psi$$

The linearized equations are:

$$\frac{\partial}{\partial t}\nabla^2 f = \nu\nabla^4 f + \nabla\psi \times \nabla^3 f + \nabla f \times \nabla^3\psi$$

This leads to the eigenvalue problem: $\lambda\nabla^2 f = \nu\nabla^4 f + \nabla\psi \times \nabla^3 f + \nabla f \times \nabla^3\psi$

Using values for ψ obtained from Unmeel Mehta's program, it is possible to solve for the eigenvalues λ on a computer. If $R < 48$, the eigenvalues should have negative real part. If R is close to 48, there should be a pair of eigenvalues

$$\lambda = a + b\,i, \qquad (a, b \text{ real})$$

Where a is close to zero. Then b will be related to the experimentally observed frequency (see [3]) at which the unsteady solution oscillates.

I used a 128 x 84 grid on an annulus, so the matrix to be diagonalized is 10584 by 10584. I have prepared a computer program to do this using the following strategy: By reducing to a coarser grid, say 32 x 24, it is practical to use the QR algorithm to compute all of the eigenvalues and corresponding eigenvectors. The only eigenvalues of interest are the ones with real parts near zero. The accuracy of these can be improved by going back to a finer grid and using an iterative method such as the Wielandt method (see [2]). Preliminary results indicate that this strategy is feasible, but so far numerical instabilities have prevented getting results accurate enough to compare with experiment. I hope to be able to complete the project next summer.

References

[1] Mehta, U. B., Dynamic stall of an oscillating airfoil. AGARD proceedings no. 227.

[2] Nakamura, S., Computational Methods in Engineering and Science. Wiley, New York, 1977.

[3] Nishioka, M. & Sato, H., Mechanism of determination of the shedding frequency of vortices behind a cylinder at low Reynolds numbers. J. Fluid Mech. (1978) vol. 89 part 1 pp.49-60.

[4] Telionis, D. P., Unsteady Viscous Flows. Springer-Verlag, New York, 1981.

Numerical Calculations of Magnetic Braking in Protostellar Clouds

E. Howard Scott

Queen's University
Kingston, Ontario
Assistant Professor of Physics

I have made considerable progress in the effort to model magnetic braking in protostellar clouds. I have adapted the 3D numerical hydrodynamic computer code of Tohline (1978) to include the effects of magnetic fields.

I had earlier modelled magnetic clouds in 2D using a vector potential representation of the magnetic field. This commonly used method is not applicable to non-axisymmetric field geometries, so that another approach had to be devised. This method, called the "FLUX" method, relies on the principle of conservation of magnetic flux through any surface comoving with the conducting fluid. Individual fluxes through elemental areas defined in each computational cell are used to represent the field. The advantage of FLUX is that it is very similar to the "donor-cell" method of the Tohline code for transport of the various physical quantities such as mass density, momentum density, etc., and thus is well adapted for inclusion in this code.

FLUX had earlier been tested in a 2D version and proved satisfactory. This summer FLUX was used in a 3D version, which required much more complicated coding, thus requiring extensive "debugging." The aim was to reproduce an earlier 2D simulation of a collapsing magnetic cloud. This provides a crucial test which the 3D code must pass in order for any later results to be trusted.

The accompanying graph shows the results of this test run. Shown is the run of central magnetic field strength versus central gas density during the collapse of an initially uniform, spherical gas cloud. The evolution follows an irregular early course followed by a steady collapse with $B_{central} \propto \rho_{central}^{1/2}$ (This behavior is described in detail in Scott and Black (1980)). The solid line shows the earlier data derived from the 2D simulation. The "X's" are data points from current 3D simulation, also starting from an initially uniform spherical cloud. As can be seen, the 3D data are almost identical to the 2D data. Unlike the 2D code, the 3D one is not constrained to remain axisymmetric. However, over the whole evolution, no spurious non-axisymmetry developed to better than one part in 10^{10} using a measure that is essentially $(\Delta\rho/\rho)$ non-axisymmetric. Because we are interested in precisely the detailed rotation history of the clouds this excellent performance on the test case is very encouraging.

Having successfully reproduced earlier 2D simulations, the 3D code is now ready to be used to attack problems with both rotation and magnetic fields, in particular magnetic braking of the protostellar clouds.

References

1. Scott, E.H., and Black, D.C. 1980, Ap. J., 239. 166.

2. Tohline, J.E., 1978. PhD Thesis, Univ. of Calif., Santa Cruz.

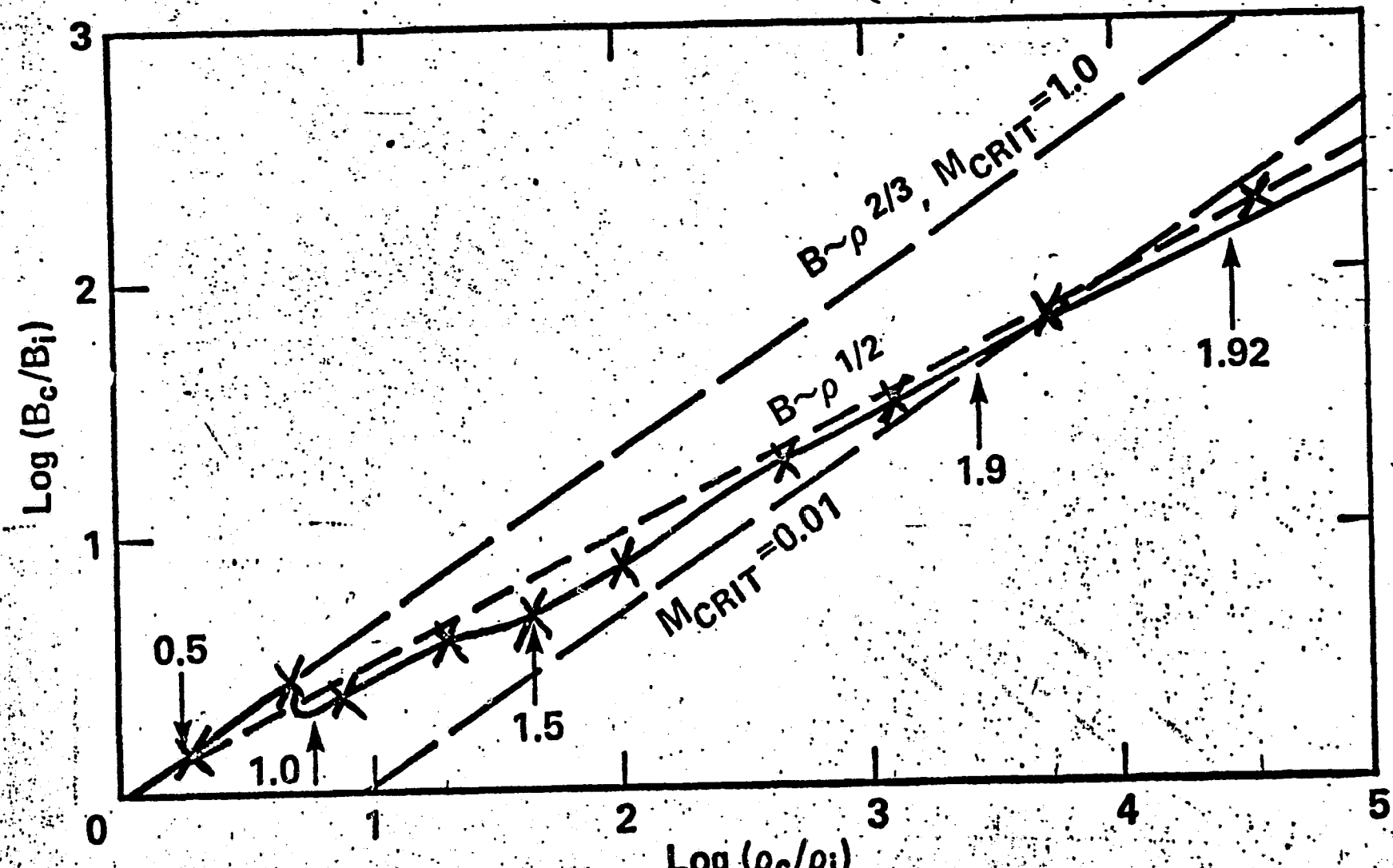

INVISCID TRANSONIC FLOW: INVESTIGATION OF NONUNIQUENESS AND INCORPORATION OF CONVECTING VORTICES

Final Report - Abstract
1982 NASA/ASEE Summer Faculty
Fellowship Program-NASA-Ames

John Steinhoff
University of Tennessee
Space Institute
Tullahoma, TN 37388

During the course of the program, two topics related to inviscid transonic flow were investigated. The first involved determining the possible existence of limit cycles in unsteady potential solutions and the existence of multiple steady Euler solutions for two dimensional transonic flow over airfoils. The second topic involved the inclusion of convecting vortices in three dimensional transonic potential flow.

In the first investigation, computer runs were first made with an unsteady small disturbance computer code, LTRAN2, developed by Peter Goorjian and William Ballhaus of NASA-Ames.[1] These runs were made to investigate the time-dependent behaviour of solutions for flow similar to that in which multiple steady solutions were found.[2] The steady solutions, for symmetric airfoils at zero angle of attack, consisted of a symmetric - zero lift one and two mirror-image non-symmetric lifting ones. The first study showed that the symmetric solution was the unstable one. Fig.1 shows how lift increases with non-dimensional time after a small transient, for one quarter time period, perturbed the initial, symmetric flow. This result has implications for transonic buffetting where the physical flow does not reach a steady state but continues to oscillate. Our results indicate that if due to boundary layer or other physical effects, the non-symetric solutions are unstable, then the entire flow will be unstable. The time units in the figure correspond to one period (observed experimentally) for buffetting for a similar airfoil. The slow growth of the computed instability compared to the physical phenomenon indicates that another physical effect not included in the calculation, such as boundary

layer growth, may be responsible for the observed rapid oscillations. Also, self - sustained oscillations were not seen in the computed results and the unsymmetric solutions appeared to be stable, futher indicating importance of other effects such as boundary layer growth in buffetting.

A second part of this study involved the steady Euler equations. A series of computer runs was made using a two-dimensional Euler Equation solver developed by Thomas Pulliam and Joseph Steger,[3] to determine whether non-unique solutions exist for the Euler equations. A systematic method for investigating this question involves determining the amount of lift induced by a small angle of attack as a function of Mach number. Results in Ref. 2 indicate that this quantity becomes singular at the bifurcation point where multiple solutions appear. Preliminary results indicate that, for Euler solutions, this quantity is not singular, at least until Mach numbers are reached for which the code fails to converge. This convegence failure may indicate lift divergence. Further investigation of this question is required.

The second main topic involved embedding a convected vortex in a three-dimensional rapidly converging potential flow code.[4] The test case computed involved convection of a line vortex past a wing, where a weak shock was induced. The rapid convergence of the code was not affected by the presence of the vortex.

REFERENCES

1. W. F. Ballhaus and P. M. Goorjian, "Implicit Finite - Difference Computations of Unsteady Transonic Flows About Airfoils," AIAA Journal Vol. 15, Dec. 1977, pp. 1728-1735.

2. J. Steinhoff and A. Jameson, "Multiple Solutions of the Transonic Potential Flow Equation," AIAA Paper 81-1019, AIAA 5th Computational Fluid Dynamics Conference, Palo Alto, Ca., June, 1981.

3. T. H. Pulliam and J. L. Steger, "On Implicit Finite-Difference Simulations of Three Dimensional Flow," AIAA Journal Vol. 18, Feb. 1980, pp. 159-167.

4. J. Steinhoff, "The Treatment of Convected Vortices in Compressible Potential Flow," University of Tennessee Space Institute Report, 1982.

DEVELOPMENT OF [illegible]

$M_\infty = .79$, 18% THICK AIRFOIL

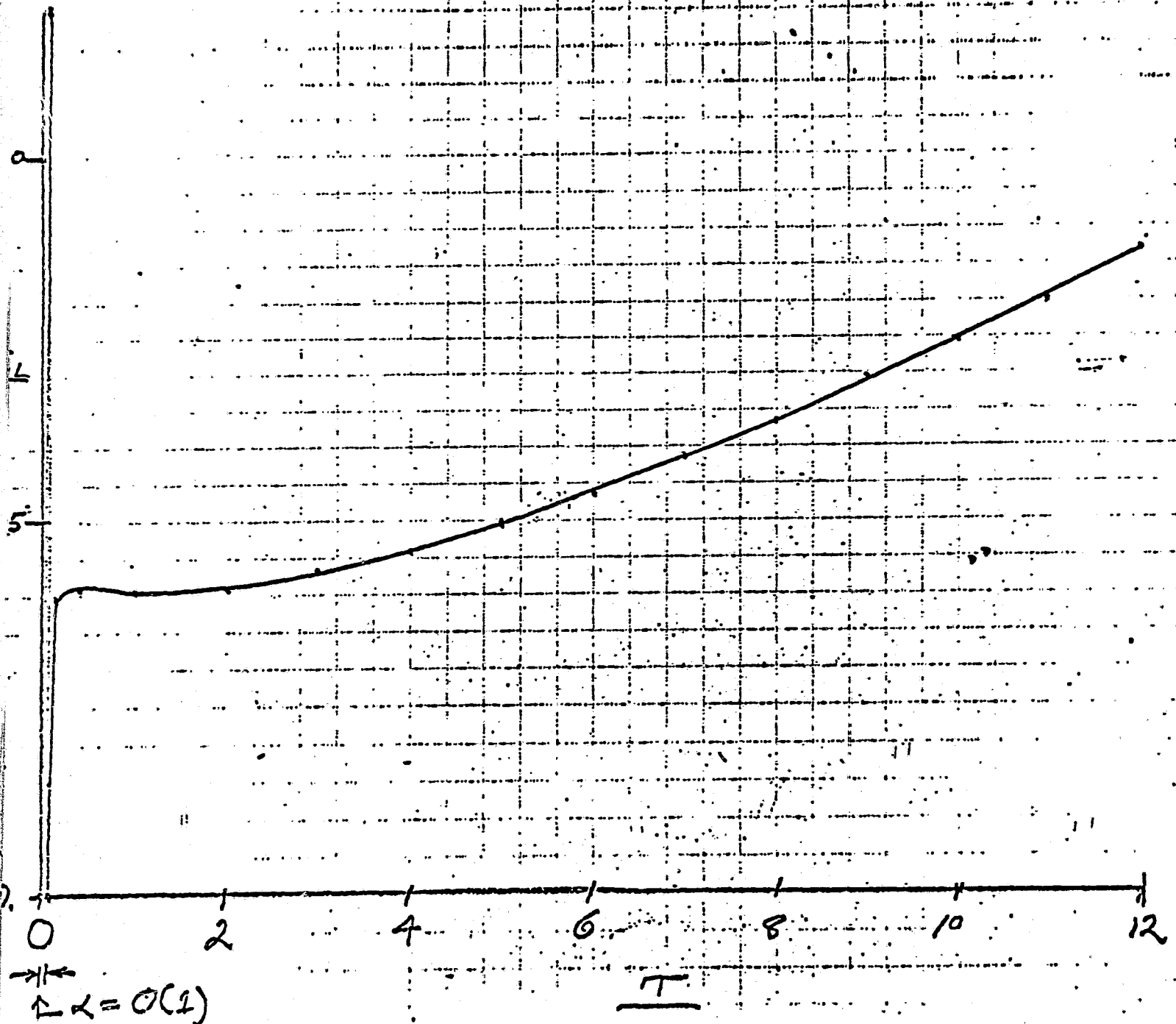

ISOTOPIC RATIOS IN SPACE DUST AND ATMOSPHERIC AEROSOLS

Allen B. Tucker
Physics Department
San Jose State University

At MeV energies, individual nuclei can be counted and the size of the pulse produced is a measure of the nuclear charge. Thus mass spectrometry with nuclear particle accelerators is capable of very high sensitivity (assays at 10^{-12} - 10^{-15} ratios of desired-to-background isotopes have been reported) with small samples (about 10^{8} atoms are needed in a sample for a measurement with 1% counting statistics). This summer I have done preliminary work on application of this new technique to two NASA/Ames research programs.

First is analysis of "space dust". As it moves about the sun, the earth sweeps up interplanetary dust. In contrast to meteors, small particles (about 10 microns) can radiate the energy associated with their cosmic velocities rapidly enough to survive the capture essentially unaltered. Collected in the stratosphere on U-2 aircraft with minimum terrestrial contamination, they are a record of the composition of the early solar system. I am developing a proposal for isotopic analysis of selected light elements at the new NSF-U. of Arizona accelerator mass spectrometry facility. A preliminary test of ion source output from a 20 mg sample of the Murchison meteorite was conducted in August. Beams of 10^{11} particles per second of the abundant stable isotopes were produced.

A second application is measurement of cosmogenic Be-10. Radioactive Be-7 and Be-10 are produced in the stratosphere by cosmic rays and adsorbed on aerosol particles. With half life of 53 days, Be-7 activity can be counted by conventional gamma-ray spectroscopy. The 1.6 s 10^{6} yr half life of Be-10 makes decay counting impractical. However the Be-10 inventory in samples of the size collected by

the U-2 aircraft can readily be counted by accelerator mass spectrometry. Since the short-lived Be-7 activity will tend exponentially toward saturation (decay rate equal to production rate), ratios of Be-7/Be-10 would be a measure of stratospheric residence times for the air masses sampled. The new NSF-U. of Arizona facility has not yet measured Be-10. However labs at U. of Pennsylvania, Orsay, and ETH Zurich (with which I have contact) have experience with this isotope. A proposal for Be-10 counting of aerosol samples is being written.

Electron Extraction and Attendant Processes Induced by Ions Incident on Crystalline Metallic Surfaces

I. Harold Zimmerman

Assistant Professor of Physics
Clarkson College
Potsdam, New York 13676

The investigation undertaken this summer is the first stage of a rather ambitious program of research aimed mainly at understanding how electron transfer takes place when a positively charged ion is neutralized during encounter with the surface of a metal. Eventually I hope to include nuclear recoil, lattice dynamics and some electronic structure effects in the model, but for the present a very simple approximation to the system is being employed. This still should suffice to demonstrate the basic neutralization process and to give some indication of how free electrons can be produced by the ion impact. Understanding these two phenomena, electron transfer to the ion and the production of free electrons, is the principal goal of the present stage of research.

The metal is represented by an unidifferentiated, positively charged "jellium" that occupies the left half-space. The negative x-axis lies within this jellium, with the origin at the jellium surface and the positive x-axis extending into the vacuum. The surface thus coincides with the y-z plane. Ion bombardment is represented by a point charge of magnitude +q moving toward the surface with a specified velocity along the x-axis. The cloud of conduction electrons associated with the metal is modeled in accordance with the density functional formalism[1] as a charged quantum fluid whose charge density is equal to that of the jellium deep in the bulk. Nearer the surface, the electron "fluid" decreases in density and extends into the region of positive x owing to its self-repulsion. Within this model there is clearly no possibility of representing lattice dynamics; the lattice has been smeared out into a uniform background of positive charge. This, in turn, means that the trajectory of the incident ion cannot be ascertained from the dynamics of the model. It must be prescribed. That will do for the present, however; our first interest is in the electronic response to the impact. Our simple model lets us address several relevant questions: (1) Are collective electron effects important? (2) Is the neutralization accomplished principally by Auger-assisted transfer to the incident ion's neutral ground state, or by quasiresonant transfer to excited levels of the ion? (3) If Auger transfer dominates, does it manifest itself by means of convoy electrons traveling in train with the receding (neutralized) ion, by means of excitation within the electronic fluid that remains associated with the metal, or by some combination of these?

The energetics of (quasi-) resonant and Auger-assisted electron transfer are sketched in Fig. 1. (Quasi-) resonant transfer can easily be a one-electron process, but Auger transfer must involve at least two electrons and possibly more. A reasonable scenario for Auger-assisted transfer involving the production of both convoy electrons and internal excitation within the metal is indicated in Figure 2. This figure also suggests how the results of these calculations might best be displayed: by means of computer-generated motion pictures portraying the evolution of the electronic fluid under the stimulus of the ion impact. The computer program is therefore designed to facilitate eventual translation of the output data into graphic form.

Initially, a 1-dimensional approximation is made whereby the complexity of the calculation is greatly reduced as is the time needed for a run. These reductions let us try out a number of computational schemes so that the most suitable approach will be evident before any large investment need be made. Within the program the electron density amplitude function is represented using the finite element method in conjunction with the Raleigh-Ritz-Galerkin variational procedure[2]. The functional is written as

$$J = \int dt \int dx \; \Psi^* \left[i\hbar \frac{\partial}{\partial t} - H \right] \Psi \; ,$$

where Ψ is the density amplitude function and H is a local approximation to the multi-electron hamiltonian operator[1]. The ranges of the integration are assumed to be such as to justify the assumption that Ψ never changes on the boundary during the times of interest. Within the region of interest, Ψ changes in such a way as to render J stationary.

The problem is nonlinear because H depends on Ψ. This leads to a number of challenging difficulties that have taken up most of the summer's effort. These seem now to be largely in hand, and the program can profitably be transferred to the Clarkson computer system when I return there. By next summer I expect to have finished work on the present 1-dimensional model system and to have the full 3-dimensional calculation ready to run. Treatment of nuclear dynamics should also be ready to begin at that time, represented by the addition of a lattice core ion positioned at the impact site.

REFERENCES

1. F. Garcia-Moliner and F. Flores, Introduction to the Theory of Solid Surfaces (Cambridge University Press, New York, 1979).

2. K.-J. Bathe and E. L. Wilson, Numerical Methods in Finite Element Analysis (Prentice-Hall, Englewood Cliffs, 1976).

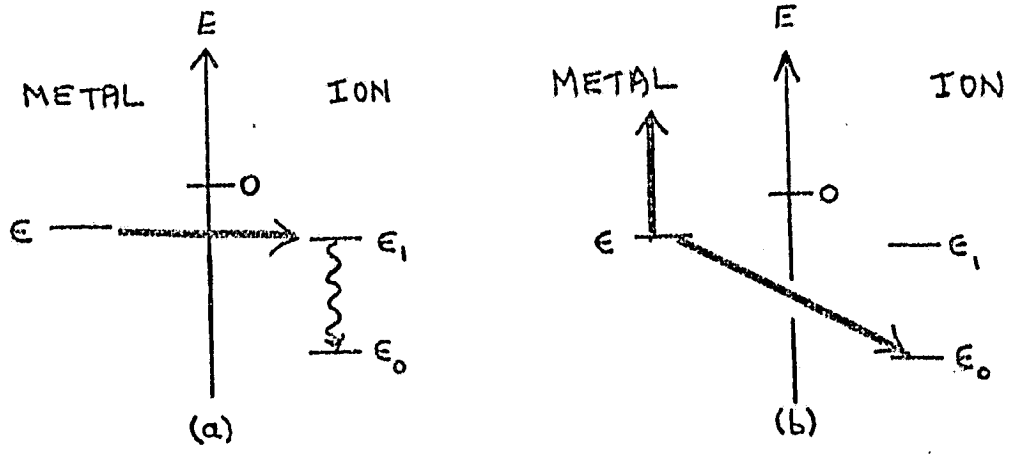

Fig. 1

(a)(Optically assisted) quasi-resonant transfer. A conduction electron jumps from the metal to the ion's excited state of energy ϵ_1, and subsequently decays to the ground state by emitting a photon.

(b) Auger assisted transfer. An electron jumps to the ion's ground state, giving up energy to another electron as it does so. The second electron may be sufficiently excited as to escape entirely.

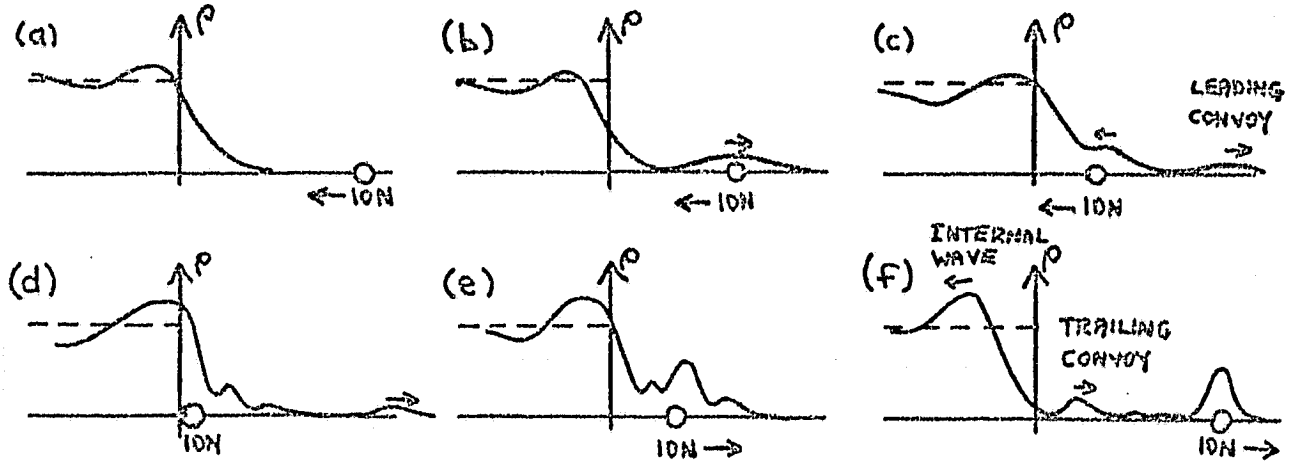

Fig. 2: An Auger-assisted transfer — schematic representation. The dashed line indicates the positive jellium density ρ_+; the solid line gives the conduction electron density. Probability pulses are identified with convoy electrons, internal excitation waves within the metal, or the neutralizing (transfered) electron.

1982

ABSTRACTS

SECOND-YEAR FELLOWS

Dictyostelium discoideum, an Ontogenetic Model for the Study of Bio-Gravitational Effects on Cellular to Organismic Programmed Development, Including Senescence and Death

Morris Aaron Benjaminson

Long Island University College of Pharmacy & Health
Associate Professor of Public Health

Knowledge of the unique life cycle and strategic evolutionary position of Dictyostelium discoideum prompted me to suggest it as a candidate for free fall experimentation in a response I submitted to the first solicitations for life science experiments to be flown aboard the Space Shuttle.

This organism begins its career, upon emerging from a spore, as an independent, actively feeding and dividing myxameba. Its food consists of bacteria. After feeding and cell division have simultaneously ceased, certain myxamebae send out pulses of chemical signal (hormone) which, upon contacting other amebae, cause them to elaborate pulses of the same chemical messenger (cyclic adenosine monophosphate) and to migrate in the direction of the primary signal. These amebae become secodary sources, their target cells, in turn, become tertiary sources, and so on (1). The migrating cells clump together to form an aggregate which undergoes a series of morphogenetic movements with concomitant cellular differentiation to form an upright structure erected at a 90^0 angle to the substrate. This stage is called a papilla. The papilla then lies down upon the substrate forming a grex (slug) which migrates for a period of time. It then becomes stationary and undergoes sub-cellular and gross morphological reorganization to a sorocarp. This consists, mainly, of a slender, tapering stalk bearing at its apex a clump of spores. These are disseminated and repeat the life cycle.

All of these events are under genetic control. Gene action is modulated by intrinsic and extrinsic environmental factors. The substrate (agar, in the laboratory) should be thought of as an integral part of the organisms' functional anatomy since antagonistic, hormone-like substances reach their target cells by diffusion through the interstices of the agar lattice. Depending upon genome and environment, the life cycle is completed in from five to seven days.

My experiments have been done on the ATCC-Raper and CB wild type strains of D. discoideum. I have used the standard tools for determining gravity effects, the clinostat and the centrifuge. There is an on-going debate as to the validity of considering rotation on a clinostat a means of nullifying the effect of the gravity vector (2,3,4,5,6,7). Salisbury (4), however, based upon observations on the space flown and Earth experiments, states, "the clinostat simulates free fall at the cellular level in many important respects." There is, on the other hand, little doubt that increased gravitational force results from centrifugation. The results of my clinostat experiments are, in summary: (1) Rotation of cultures in a range of RPM's with the substrate parallel to the gravity vector, decelerates development and produces a larger number of organisms when compared with static horizontal controls, regardless of inoculum stage (spore or myxameba) and genotype, bearing in mind that CB's rate of development is, under standard conditions, slower than ATCC's. (2) Rotation of cultures with the substrate perpendicular to the gravity vector decelerates development and often shows fewer organisms than do horizontal controls. (3) Inverted, static plates, with agar surface facing downward, show accelerated development relative to static cultures incubated with the agar surface facing upward. Inverted and rotated plates develop even more rapidly. (4) Non-rotating cultures maintained with the agar surface parallel to the gravity vector, usually show decelerated development and an increase in numbers of organisms when compared with horizontal

controls. Rotation of similarly oriented cultures decelerates development to a greater degree, but shows no numerical differences when compared with controls.

Thus, two independently acting mechanisms seem to be involved. One affects passage from stage to stage (cell to cell adhesion, perhaps) and the other, possibly the rate of cell division. So far, I have not observed the speed of rotation effects seen by Tremor and Souza (?) for animals and by others (3) for plants. However, the observation that inversion affects development in amphibian eggs (2) and the rate of slug to sorocarp conversion in D. discoideum (4) is consistent with my findings and expectations, since the force of gravity is obviously at work here. Differences in developmental rates and reactions to rotation on the clinostat in more or less related organisms (such as the ATCC and CO wild type strains) have been reported before (2). Relative prox motility is under genetic control (9,10). I have observed this in comparing the effects of illumination on prox migration in ATCC vs. CO wild type strains. Therefore, so is the point in time of the slug to sorocarp transformation.

If free fall and clinostat treatment can be equated, the logical question becomes, "Where, in developmental time, does free fall act?" My data, so far, indicate between 0 and 40 hours after the spore inoculum has been placed on the medium. Experiments are currently under way to further narrow the time span. There is disagreement as to whether free fall can have an effect on a cell below 10µm across (11,12). D. discoideum spores range from 6-9µm in length, while the amebae are 5.5 to 16.5µm across. Therefore, if there is, indeed, an effect on the level of the individual cell, it is probably on the myxameba. The cell aggregation phenomenon is another likely target within the 0-40 hour time frame.

Centrifugation of cultures started from amebae on the NASA-UCSC Botanical Centrifuge (13) at 5.7% and 10 g indicate deceleration of development at a time which could correspond to the approach to slug transition. Cultures begun with a spore inoculum, centrifuged on the 12 foot radius instrument (NASA-Ames) at 3 g showed effects which indicate that this treatment accelerated either the rate of cell division or of development, in general. Unfortunately, the relatively crude methods I have available create, in my mind, some uncertainty concerning the data obtained, as the numbers are small. I have an experiment started from an ameba inoculum on the centrifuge, now.

In a search for a candidate statolith(s), mitochondria (14,15) among others, have been suggested. Bacteria are present in the feeding myxamebae and are similar in dimensions to mitochondria. In those cultures developing motionless and on edge, the increase in the number of individuals could be the result of a sedimentation of bacterial particles, contained in vacuoles, which upsets the cytoplasmic equilibrium triggering the cell to divide. This possibility could also explain similar results in cultures rotated parallel to the gravity vector as contrasted to those rotated similarly, but perpendicular to the gravity vector; i.e., decelerated development not necessarily coupled to increased numbers of individuals. This is in keeping with the suggestion (4) that morphogenetic responses (such as pre-aggregative switching) could be altered by cytoplasm-vacuole interactions.

An inspection of the Space Shuttle Flight Manifest, issued 4/14/82, shows that all of the six Life Science Space Lab flights (9/83-4/87) will last for 7 days. The D. discoideum life cycle fits into this schedule perfectly. The fact that Payload Specialists/Scientists will be crew members means that the entire experiment, from culture incubation to data recording can be carried out in space with no danger of launch or re-entry artifact. My survey of flight-related documents and

literature included descriptions of BIOSATELLITE II, DISCOVERER XII,XVII, SKYLAB 3,4, GEMINI 3,11, NERV I, APOLLO-SOYUZ, APOLLO 16,17, [illegible] COSPAR volumes, KOSMOS reports, etc. A space flight effect which has been noted in diverse biota, ranging from microbes to insects to plant material to fish eggs, is a change in the rate of the genetically programmed life cycle relative to that of Earth controls. D. discoideum's life cycle: emergence, feeding and growth, cell differentiation, reproduction/senescence, death, lends itself to studies of developmental rates. Last year, at Ames, in preliminary studies with the fluorescent vital dye, 4-acetamide-4'isothiocyanostilbene 2,2' disulfonic acid (SITS),(16) I was able to demonstrate a lack of toxic effects throughout the Dictyostelium life cycle and to differentiate, based on the dye's staining properties, between living and dead D. discoideum cells. SITS provides sensitive, accurate means for monitoring the entire life cycle of the organism. Katz (17) has pointed out the analogies between the developmental program in D. discoideum and that in developing embryos. The time span in Dictyostelium is, in most cases, shorter. Pollard (11), based on his calculations, believes that studies on developmental systems greater than 1 mm would be both promising and interesting. D. discoideum is a developmental system which achieves this minimum size and beyond, goes through a complete developmental life cycle in 5-7 days which is similar to divergent life forms, and includes an analog of embryogenesis in its programme. It is, therefore, an ideal candidate for experiments in SPACELAB. The instrumental parameters for integrating D. discoideum experiments into the SPACELAB configuration can be easily determined through use of a device such as the Plant Carry-On Container (PCOC) in its designated role in a test similar to the HEFLEX Bioengineering Test (HBT) (18).

REFERENCES

1. Tomchik, K.J. and Devreotes, P.N. 1981, Science. 212:443-446.
2. Tremor, J.W. and Souza, K.A. 1972. Space Life Sciences. 3:179-191.
3. Gordon, S.A. and J. Shen-Miller. 1966. in Brown, A. H. and M. Florkin (eds.) Life Science and Space Research IV. Spartan Books, Washington, D.C.
4. Salisbury, F.B. 1969. BioScience. 19:407-410.
5. Tibbitts, T.W. and Hertzberg, W.M. 1978. Plant Physiology. 61:199-203.
6. Brown, A.H. 1979. The Physiologist. 22:S15-18.
7. Brown, A.H., Dahl, A.O. and Chapman, D.K. 1976. Plant Physiology. 58:127-130.
8. Bonner, J.T. and Shaw, M.J. 1957. J. Cell. & Comp. Physiol. 50:145-153.
9. Keyman, S.C. and Clarke, M. 1980. J. Cell Biol. 87:327A.
10. Sussman, M., Schindler, J. and Kim, H. 1978. Exp. Cell Res. 116:217-227.
11. Pollard, E. C. 1965. J. Theoret. Biol. 8:113-123.
12. Tobias, C.A., Risius, J. and Yang, C.H. 1973. COSPAR XI:127-140.
13. Brown, A.H., and Chapman, D. K. 1977. Plant Physiology. 59:636-640.
14. Shen-Miller, J. and Hinchman, R.R. 1974. BioScience. 24:643-651.
15. Sievers, A. 1971. in Gordon, S.A. and Cohen, M.J. (eds) Gravity and the Organism. The University of Chicago Press, Chicago and London.
16. Benjaminson, M. A. and Katz, I.J. 1970. Stain Technology. 45:57-62.
17. Katz, E.R. 1978. BioScience. 28:692-697.
18. Brown, A.H. and Chapman, D.K. NASA brochure.

DISPLAY REQUIREMENTS FOR REMOTELY PILOTED VEHICLES

Barbara A. Dernabe
Florida Institute of Technology

A fair amount of attention at Dryden Flight Research Facility has focused on the functional, operational, and handling characteristics of remotely piloted vehicle systems (RPV). In such a system, a pilot controls an aircraft from a ground based cockpit in either a full manual or coupled control mode.

The information available to the pilot for flying maneuvers such as spin initiation, spin recovery, and approach and landings is limited to instruments and a TV moniter which displays a video image transmitted from a camera mounted on the aircraft. This presumably provides a pilot's eye view of the world.

To illustrate, one such system is the HIMAT, acronym for highly maneuverable aircraft technology. It is a 3/8 scale model flown from a ground based cockpit. Such a system raises a number of serious issues with respect to human information processing, manual control, and pilot workload demands. On the one hand, unlike a simulation there is something at stake. While not life threatening, a serious error could crash the aircraft -- not to mention crush the pilot's ego. On the other hand, flying an RPV is something like doing an impoverished simulation, eg. in a fixed based simulator, since many of the cues present in flight are unavailable in the ground based cockpit.

PERCEPTUAL CONSIDERATIONS

1. Cockpit Layout - Since there is no size constraint, the cockpit instrument layout is spread out, thus increasing the necessary eye and head movements of the pilot.

2. Vestibular/Proprioceptive Cues - Cues to orientation in space are absent. This in itself is not unmanageable since visual cues can often override or substitute for these. However, in RPV flights visual cues are also impoverished.

3. Limited Visual Field - The pilot's visual field is constrained to a 19 " TV moniter presenting a 24 degree horizontal and 14 degree vertical field of view. This poses two kinds of problems. A) Specifically in approach to landing, it can distort perception of position with respect to the runway when the aircraft is banked or in crosswind conditions. In fact when heading is corrected for crosswind the runway may actually fall completely outside of field of view. The same is true for steep approaches where the horizon may fall outside of field of view.

B) A limited field of view also results in an elimination of peripheral vision which supplies important motion cues that in turn contribute to perception of altitude and airspeed. This happens because objects appear to move more slowly across the visual field than nearer objects. The pilot typically uses this subtle information in his assessment of altitude.

Current research at Dryden includes a wide angle video system provide 160 degrees field of view and limited resolution

peripheral vision.

4) Resolution - Resolution of TV transmission is poor and sometimes transmission is lost altogether during flight. This has a particularly dramatic effect during approach and landing.

5) 3-D Information - The pilot is looking at a flat picture which does not activate the oculomotor cues of accomodation, convergence, and binocular disparity, which are important for depth and distance perception.

In fact, all the pilot has available is 1) the horizon and runway which provides some pitch and roll information, 2) changing runway perspective which provides some altitude cues, and 3) minimal velocity and texture gradient which provides some altitude information during approach. However, since the runway and its surround are homogeneous even these cues are impoverished. Also while it is true that pilot's have instrument information in addition to the video information they are a general reluctant to take their eyes off the TV to refer to the instrument display. Often this results in reliance on the control engineer for altitude and airspeed callouts. As a result flying RPV's is considered a very high workload task. The human factors problem is thus to facilitate performance and reduce pilot workload.

TASKS

1) Assess parameters critical to performance
2) Ascertain the information impoverished or absent in the video display.
3) Provide that information in an alternative manner.

RESEARCH DIRECTIVES

A clear alternative for presenting information to the pilot is through the use of an integrated head up display. In a study conducted by the author last summer, the following display characteristics were seen as critical: 1) focal presentation, 2) task specific flexibility, 3) relative status, and 4) control input guidance. A display possessing these characteristics and currently undergoing tests at Ames Research Center is a conformal head's up display developed by Richard Bray. Elements of the display include a horizon, runway, heading indicies, attitude indicator, flare cues, and steering commands for holding glideslope and localizer. Proposed modifications of the display for RPV flights are being coordinated with Dryden software engineers for future tests on Dryden's new Evans and Sutherland graphics system.

GRAVITATIONAL EFFECTS OF THE ASSOCIATION,NGC 206, ON THE DISK OF THE ANDROMEDA GALAXY

Gene G. Byrd. Associate Professor of Astronomy, University of Alabama

The galaxy M31 has a two-armed spiral pattern in its disk. Recent 21 cm observations by Unwin[1] show the hydrogen gas structure of the disk of M31 with improved resolution. The main spiral arms can be seen in the observations, but there are a number of irregularities. In particular, a steeply pitched "armlet" extends along the southwest semi-major axis of M31's tilted disk between the two major arms (see figure 1).

My project has been an attempt to explain this structure. Photographs of M31 show a large star cluster, NGC206, at the inner end of the armlet (figure 1). My hypothesis was that the armlet and other nearby disturbances are caused by the gravitational effect of NGC206. I intended to quantitatively verify this using computer simulations of NGC206 orbiting in the disk of M31.

Last summer was spent on two approaches to this project. I worked on developing a program for a first, simpler, approach to the problem. The second approach, more realistic but more complicated, involved modifying a program by R. H. Miller and B. F. Smith (my NASA colleague). During this last winter, I continued work on the simpler approach and submitted the first version of an article describing the results to The Astrophysical Journal.

During this summer, I have completed the simple approach computer runs and written the final version of the article which has been accepted for publication in the Jan. 15, 1983 Astrophysical Journal. The results of the simpler approach showed that less extensive modifications than previously planned would be sufficient in Miller and Smith's program. I have finished these modifications and am doing computer runs for the more realistic simulations. The article results show that NGC206 can create the armlet by its gravitational effect on material in the disk of the Andromeda Galaxy. These results have wider implications , supporting ideas that gravitation is the dominant mechanism for generating spiral arms in galaxies with multiple arm patterns and indicating that mechanisms involving chain reactions of supernova explosions and star formation are not important in spiral arm formation.

I will take the results of the more realistic simulations back to Alabama for analysis. Discussions with P. M. Cassen, another Ames astronomer, have raised the possibility that gravitational armlet forming processes may have been important in the much smaller scale process of forming Jovian planets in our solar system. I will investigate this interesting possibility further when I return to Alabama. Finally, I have at Alabama for furter analysis the results of simulations of collisions of elliptical galaxies by Miller and Smith.[2]

1. Unwin, S.C. 1980a, Monthly Notices of the Royal Astronomical Society vol 190,p.551
_____ 1980b, Monthly Notices of the Royal Astronomical Society vol 192, p.243
Baldwin, J.E. 1981, The Structure and Evolution of Normal Galaxies (New York: Cambridge University Press) S.M. Fall and D. Lynden-Bell eds. p.145.
2. Miller, R. H. and Smith, B.F. 1980, Astrophysical Journal vol. 235, p. 421.

Figure 1.

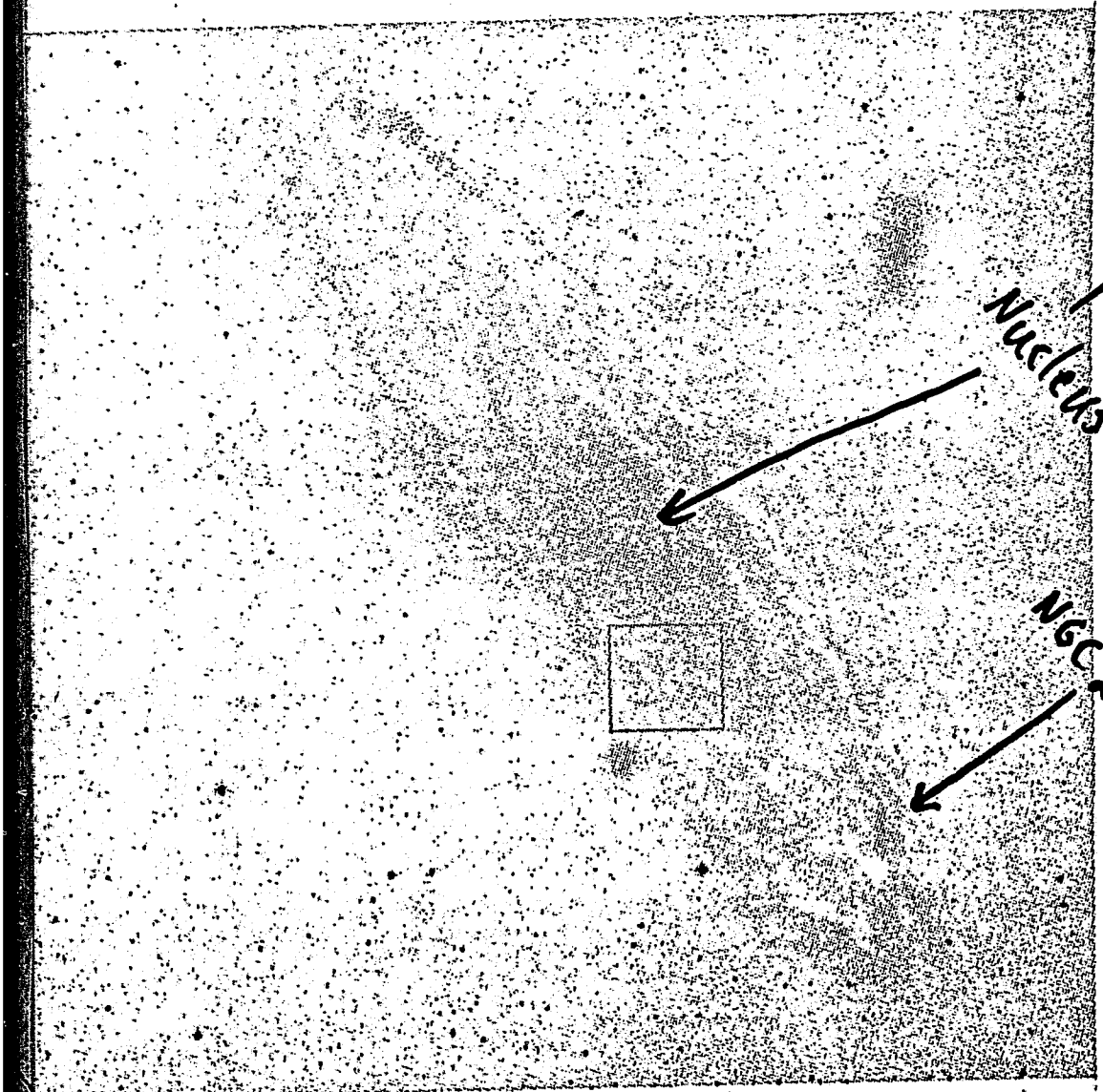

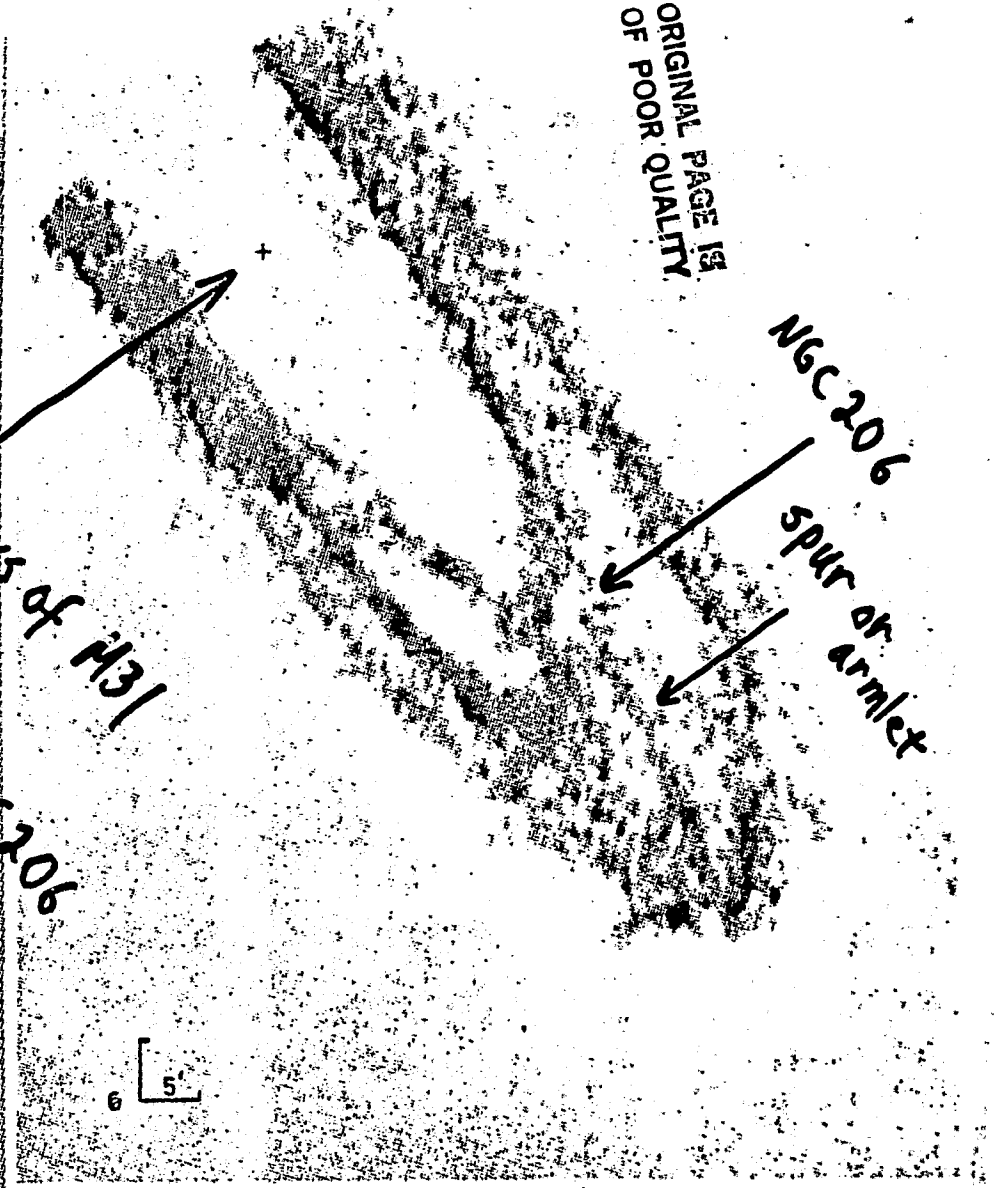

. Radio photograph of integrated hydrogen emission in the SW region of M31, at a resol of 0.8 × 1.2 arcmin. About the same scale as visual photograph.

ANDROMEDA GALAXY is arrayed from northeast to southwest n the sky above the Northern Hemisphere. Its plane is oblique with respect to the earth, so that the nearest part of the galaxy is the northern edge of its disk. The photograph shown here is printed as a negative; hence the dark parts of the galaxy consist of stars. The white parts consist of dust, which conceals the stars behind it. A prominent dust lane lies to the right of the galaxy's central bulge. The dark spot below the bulge is M32, a companion galaxy. A second companion galaxy, NGC 205, lies above and to the right of the bulge. Two other companion galaxies are outside the field of view. The diameter of this image of the Andromeda galaxy is about 125,000 light-years, and the galaxy is two million light-years from the earth. The galaxy thus subtends an angle of three degrees in the sky, or six times the angle subtended by the moon. The [illegible] The photograph was made with the 48-inch Schmidt telescope on Palomar Mountain.

Determination of Assimilatory Quotients for Chlorella pyrenoidosa 711-05 Grown in a Closed System

Arthur P. Carroll
Associate Professor
Department of Science
College of Santa Fe

In order to sustain extended manned missions in space (missions over five years), it will be necessary to develope regenerating life support systems. The CELSS program (Closed Ecological Life Support Systems) at NASA/Ames is involved in research to that end.

One of the most basic problems in sustaining life in closed systems is the need to regenerate gasses. Animals or heterotrophs consume oxygen and produce carbon dioxide, while plants, autotrophs, consume carbon dioxide and produce oxygen. In a closed system gas balances could be maintained by combining autotroph and heterotroph. Unfortunately the ratio of gas consumed to gas produced is not the same for each. The quantitative expression for the CO_2 consumed and the O_2 produced by plants is known as the Assimilatory Quotient (A_q)

A great deal of information regarding the Assimilatory Quotient of plants, especially the green algae, exists in the literature. However, most of these studies occurred in open, flow through systems rather than closed systems. In order to study the effect of closed systems on the A_q , NASA designed a closed system to accommodate growth of both an heteroph and an autotroph (Figure 1).

Before the system could be fully utilized, it was necessary to test its reliability and reproducibility. Last summer experiments were performed using the green alga Clorella pyrenoidosa 711-05. The A_q of the organism was determined in the closed system under conditions of different O_2 starting concentrations. The initial data indicated a variation in the A_q at different concentrations.

This summer experiments were performed to verify the results of last summer. It was necessary to determine the varience in results obtained at constant conditions. Six experiments were performed to determine the A_q at a starting O_2 concentation of 20%. (Table 1). It quickly became apparent that reproducible results were difficult to obtain. The initial experiments were performed at a reduced pressure (650 mm Hg initial) in a Helium background. Increases in pressure would occur during the experiments. These increases, if due to leaks in the system, would account for the variations in results. An experiment was performed in which the starting pressure of 650 mm Hg was used and the gas in the head space was monitored by means of gas chromatography. The presence of Nitogen in the closed system would indicate leakage. Nitrogen was found and the quantity present agreed with the increase in pressure. Two more experiments were run with starting pressures of 760 mm Hg. The A_q of these experiments showed closer agreement.

Because of the existence of leaks the data produced can give erroneous results. The system must be used with caution at reduced pressure. The high relative humidity in the system can cause the vacuum fittings to leak gas from the environment. The system does seem to be reliable when used at atmospheric pressure . Experiments done at 760 mm Hg, when monitored for the presence of nitrogen gas, showed none.

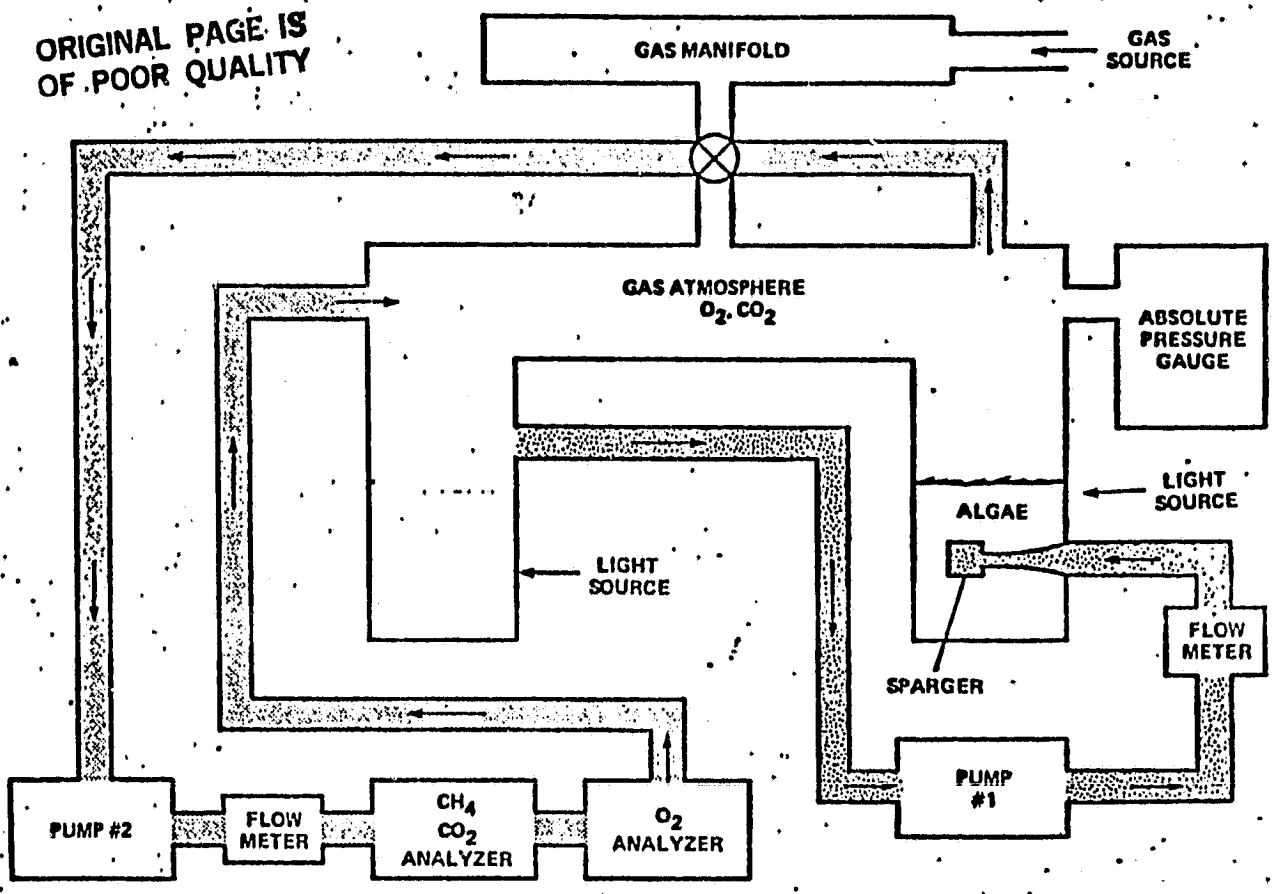

Fig. 1: Closed vessel used to grow algal culture

TABLE 1: Assimilatory quotients for Chlorella pyrenoidosa 711-05 grown in a closed system at initial oxygen concentrations of 20% and carbon dioxide concentration of 5%.

Experiment #	A_q	Starting Pressure (mm Hg)	Pressure Change (mm Hg)
1	0.72	650	70
2	0.81	650	64
3	0.68	650	83
4	0.59	760	6
5	0.57	760	6
6	0.64	650	71

References

1. Ammann, E., and V.H. Lynch. "Gas exchange of algae: I- Effects of time, light intensity and spectral energy distribution on the photosynthetic quotient of Chlorella." Applied Microbiology, 13(4): 546-551. 1965.

2. Ammann, E. , and V.H. Lynch. "Gas exchange of algae: II- Effects of oxygen, helium and argon on the photosynthesis of Chlorella." Applied Microbiology, 14(4): 552-557. 1966.

3. Badger, M.R. and T.J. Andrews. "Effects of CO_2, O_2 and Temperature ona high-affinity form of ribulose diphosphate carboxylase-oxygenase from spinach." Biochem. Bioph. Res. Commun. 60: 204-210. 1974

4. Frischnecht, K. and K. Schneider. " Physiological performance of the blue-green algae, Anacystis nidulans in a continuous turbidostat fermenter culture." Archiv. of Microbio. 120: 215-221. 1979.

5. Ogawa, T., T. Fujii and S. Aiba. "Effect of oxygen on the growth yield of Chlorella vulgaris." Archiv. of Microbio. 127: 25-31. 1980.

6. Pirt, M.W. and S.J. Pirt. "The influence of carbon dioxide and oxygen partial pressures on Chlorella growth in photosynthetic steady-state cultures." Journ. of Gen. Microbio. 119: 321-326. 1980.

Surface Structure of Vitreous Silica - A Molecular Dynamics Study

By S. H. Garofalini
Department of Ceramics
Rutgers University

The importance of vitreous silica (v-SiO_2) in catalysis, microelectronics, optical fibers, and commercial glasses is well appreciated by physical scientists working in these areas. Many of the details of the structure and dynamics of v-SiO_2 at an atomistic level must be inferred from experimental techniques which provide only average properties (e.g. X-ray and neutron diffraction, IR and Raman spectroscopy). Also, the amorphous and insulative nature of v-SiO_2 have limited the use of the more common surface analytical techniques for studying the silica surface in an unambiguous manner.

The lack of these details at the atomic level provides impetus for the application of the molecular dynamics (MD) computer simulation technique to study v-SiO_2. Once the accuracy of this technique has been established, it can be used to provide significant information into the structural and dynamic behavior of atoms in v-SiO_2 and at the v-SiO_2 surface under a variety of conditions.

The excellent computational facilities at NASA-Ames have enabled me to perform this evaluation of the adequacy of the MD technique to accurately simulate v-SiO_2. The work last summer showed that the technique accurately simulates atomic motion in bulk v-SiO_2 (1) . This summer, the work has been aimed at establishing if the surface of v-SiO_2 can be accurately simulated.

The result of the work this summer clearly indicates the adequacy of using the MD technique to study the v-SiO_2 surface. The simulations reproduced the expected predominance of the oxygen atoms (rather than silicon atoms) at the surface, as well as the occurrence of several non-bridging oxygen. An appropriate decrease in the Si-O-Si bond angle was also found to occur at the surface. The radial distribution function (RDF) as a function of distance from the surface was evaluated so as to determine the structural changes occurring at the surface. Figure 1 shows the RDF from (a) atoms in the interior of the sample (approximating the bulk), (b) all atoms within 10Å of the surface, and (c) all

atoms within 5 Å of the surface. The first peak in each RDF is due to the Si-O pairs and occurs at the appropriate bond distance of 1.62Å. The shoulder in the Si-O peak in Figure 1c was found to be due to the several non-bridging oxygen (NBO) at the surface,(see Figure 2).

This decrease in the Si-O distance between the NBO and Si as compared to the Si-O spacing for the normal bridging oxygen is very important. Previous calculations have indicated that the Si-O distance for NBO should be ~ 0.08Å less than the normal Si-O distance(2). Our simulation gives this result.

This result is significant in that it shows that the MD simulation used here accurately reproduces surface and defect properties of v-SiO_2.

In addition, a study of the motion of K atoms at the $K_2O{\cdot}3SiO_2$ glass surface immediately after fracture was simulated. Experimental studies (ion scattering spectroscopy) have indicated a higher than expected concentration of K atoms occurs on the fracture surface. Results of my simulation show that K atoms preferentially jump to the fracture surface within a few picoseconds.

References:

1. Garofalini, S. H., J. Chem. Phys. 76(1982) 3189.
2. Lucovsky, G., Phil. Mag. B, 39(1979) 513.

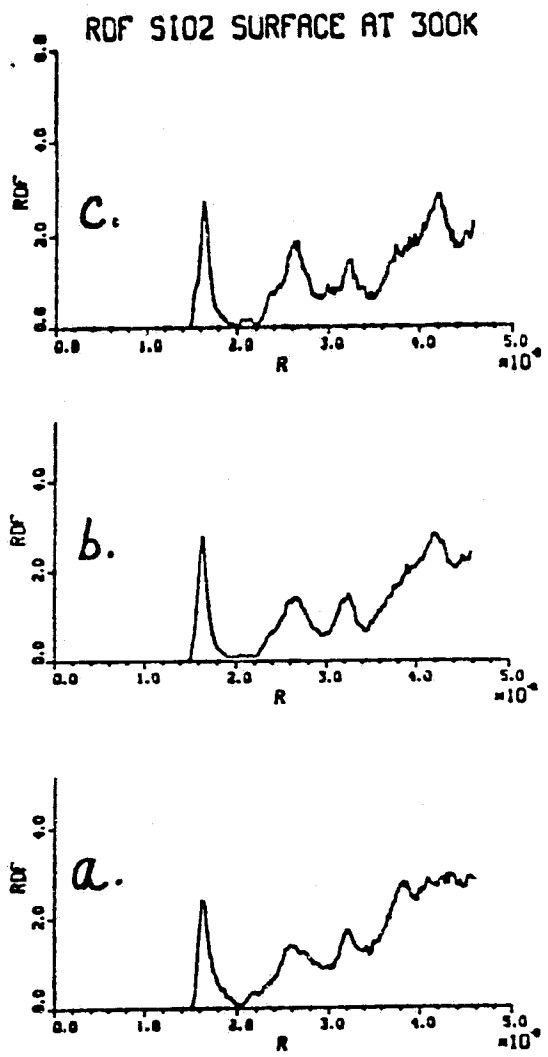

FIG. 1

a. INTERIOR

b. ATOMS FROM SURFACE TO DEPTH OF 10 Å.

c. ATOMS FROM SURFACE TO DEPTH OF 5 Å

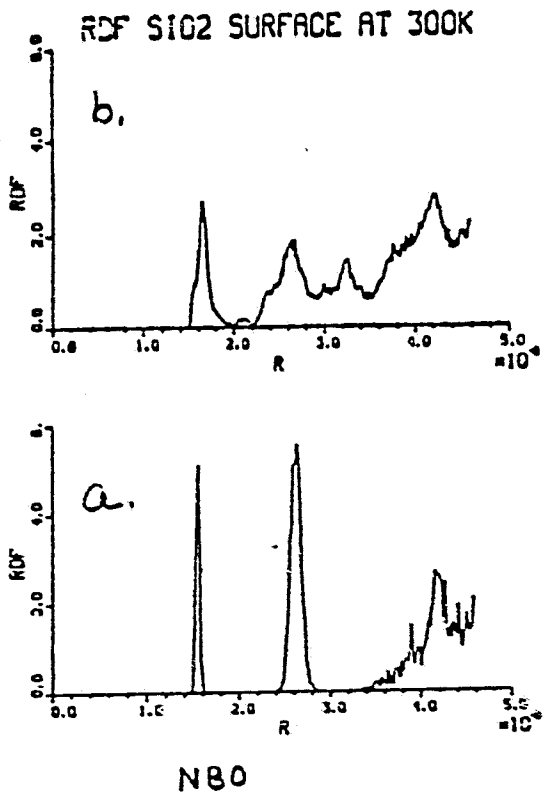

NBO

FIG. 2

a. NON BRIDGING OXYGENS (NBO) ONLY.

b. SAME AS 1c.

Aerosol Climate Effect Program-Data Comparison

Jindra Goodman
San Jose State University
Professor of Meteorology

The first project was associated with the Aerosol Climate Effects (ACE) program. It is well known that stratospheric aerosols play an important role in global climate. To assess their effect on the energy budget we have to understand their physical and chemical properties, time and space variation and evaluate the effects of major volcanic eruptions. Even though information on aerosol properties have been gathered over past two decades there remains an urgent need for simulataneous measurement using different sampling techniques. Therefore as part of the ACE program a continuous effort has been made to intercompare instruments measuring the same or similar aerosol properties. The sampling platform is the U-2 aircraft and the instruments sampling during ACE missions are listed in Table 1 along with their characteristics.

Our specific research interest concentrated on the comparison of the Ames wire impactor (AWI) with instruments, which measure similar aerosol properties (size distribution). Specifically the AWI was compared with the ASAS probe and to a lesser extent with the QCM cascade impacter. The major physical difference between the AWI and the ASAS probe is their location. The AWI is located directly in the air stream, while ASAS probe must bring a sample inside probe. To insure the representation of the sample, several conditions have to be fulfiled. Sampling should be isokinetic and isoaxial (Fuks, 1975). Detailed analyses of this condition in connection with ASAS probe indicates that there may be some problems. The original mounting hindered isokinetic flow, but recently a diffuser cone was installed to insure isokinetic conditions. The probe location on the U-2 doesn't allow isoaxial sampling. There is a very sharp bend ($\sim 90^0$) in the intake probe. This results in the loss of larger particles and the resulting errors become altitude dependent (Stokes number of particle increases with altitude). The comparison of the ASAS data with the wire impactor indicated such a trend (see Fig. 1). Additional errors in the size determination can be connected with variations in the refractive index of particles. On the other hand, sampling with the AWI depend on the collection efficiency of the wire (Lem and Farlow, 1979), sampling volume and the analytical procedure to determine particle size.

Detailed examination of data from the ASAS probe and AWI yield relatively good agreement, if we take into consideration that a 10% uncertainty in particle size will yield a 30-50% error in concentration.

Aerosol mass data obtained using the QCM cascade impactor didn't agree well with the AWI. This may be due to the fact that the size intervals are larger and the particle size is determined by a 50% collection efficiency. Summary of the data are presented in Table 2.

The second research activity involed the preparation of a proposal to study the neutralization of tropospheric acid aerosols by ammonium and their participation in the nucleation processes and connection with acid precipitation.

References:

N. A.Fuks, 1975: Review papers-Sampling of Aerosols. Atmos. Environment, vol. 9, p. 697-707.

M. Y. Lem and N. H. Farlow, 1979: Efficiency of Aerosol Collection on Wires Exposed in the Stratosphere. NASA 81147, 28 pp.

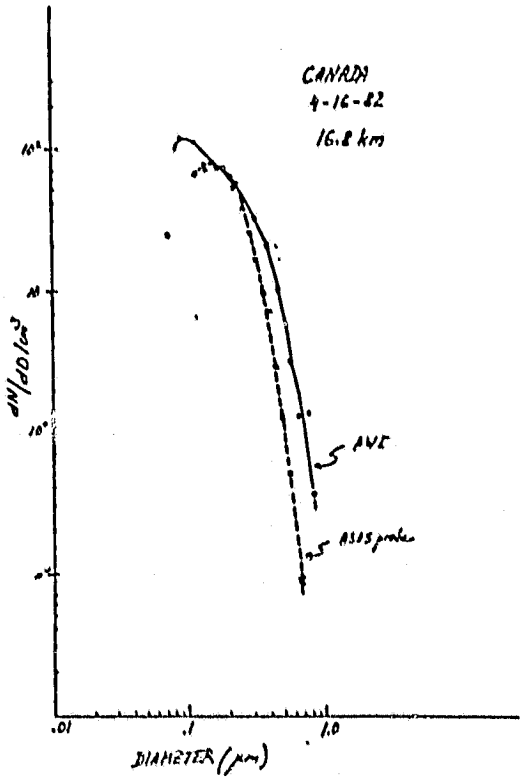

Fig. 1.

TABLE 1

INSTRUMENT	ACTIVE SCATTERING AEROSOL PROBE-ASAS	CONDENSATION NUCLEI COUNTER	AMES WIRE IMPACTOR AWI	QUARTZ CRYSTAL MICRO BALALNCE (QCM)	FILTER
quantity measured	aerosol concentration in 32 size ranges from .1μm dia. to 3μm dia.	concentration	concentration and size distribution	aerosol mass in 10 size ranges .05μm to 25μm	total $SO_4^=$ mass

TABLE 2

1982 ACE FLIGHTS

DATE	LOCATION	ALTITUDE KM	No/cm^3 >0.06μm	AERSOL VOLUME μM^3/CC	SO_4 MASS PPB	COMPARISION OF SIZE DISTRIBUTION OBTAINED FROM ASAS WITH AWI	COMPARISON BETWEEN QCM AND AWI
15 APRIL	BAJA CA	16.8	18.3	0.1667	1.0819	ASAS missed some large particles	no data avail. yet
15 APRIL	BAJA CA	18.3	28.9	.2587	1.6789	agree	"
15 APRIL	BAJA CA	20.7	6.1	.2656	1.7237	no data	"
16 APRIL	CANADA	16.8	18.8	.1924	1.2487	ASAS missed some large particles	"
16 APRIL	CANADA	18.3	5.1	.0860	.5581	ASAS missed some large particles	"
16 APRIL	CANADA	20.7	2.2	.1167	.7574	no data	"
19 APRIL	BAJA CA	20.7	2.5	.0718	.4659	no data	"
19 APRIL	BAJA CA	20.7	4.85	.0954	.6191	no data	"
5 MAY	BAJA CA	15.3	23.4	.0603	.3913	ASAS reads more small particles agreement on large particles	disagree
5 MAY	BAJA CA	20.7	3.6	.0340	.2206	agree	disagree
7 MAY	ROCKY MT.	16.8	23.7	.3666	2.3792	ASAS missed some large particles.	N/A
7 MAY	ROCKY MT.	18.3	12.6	.1718	1.1149	ASAS missed some large particles	agree

LIFE TESTING OF ACCUMULATOR BLADDERS (AIBS SYSTEM)

JOHN S. HILTEN

AUGUST 23, 1982

EMBRY-RIDDLE AERONAUTICAL UNIVERSITY

INSTRUCTOR - AERONAUTICAL ENGINEERING DEPARTMENT

Two Rotor System Research Aircraft (RSRA) have been built by Sikorsky for NASA. Each of these aircraft is unique in the sense that there are three flight configurations: (1) as a helicopter, (2) as an airplane (with the addition of engines, wings, and a horizontal tail, and with the removal of the rotor blades), and (3) as a compound (with the rotor blades back on). In the compound configuration the aircraft flies like a helicopter or like an airplane at the discretion of the pilot.

The basic purpose of the aircraft is to serve as a test vehicle for experimental rotor systems.

Helicopters in general are subject to a wide variety of vibrations; the most severe of these is known as the blade passing frequency vibration. The RSRA in its present configuration with five rotor blades that typically rotate at about 200 RPM generates a severe vibration at about 17 HZ. To reduce the transmission of this vibration to the rest of the helicopter the transmission is supported laterally by 4 active isolators (shock absorbers) that attenuate the vibration level. Each isolator has accumulators with bladders that separate a pneumatic section from a hydraulic section.

This research project will take 3 different bladders and life cycle them at pressure conditions normally encountered in flight for 12×10^6 cycles each; this is to verify their durability or mode of failure.

The envisioned procedure is to pressurize the pneumatic side of the bladder to 1100 psi with room temperature nitrogen and then to pressurize and cycle the hydraulic side via a controller and servo valve to 1650 psi $\pm$ 80 psi, at 17 HZ. The input to the controller will be from a sine wave generator set to 17 HZ and from the feedback pressure transducer measuring the hydraulic oil pressure. A ratio potentiometer will be used to match the two input signals. A bias potentiometer will be used to set the static pressure level and a gain potentiometer will be used to set the level of the pressure modulation. A dither control and limit control will also be provided. The output of the controller will be fed into the input of the torque motor which will mechanically position the pilot spool valve in the servo valve. A 3000 psi hydraulic pump with a maximum flow rate of 31 gal./min. will furnish the pressure for the servo valve. The controller, torque motor, servo valve, and hydraulic pump are available commercially.

It is desirable to shut the system down automatically in the event of a bladder failure or any other malfunction in the system. Since the system pressure is servo controlled, some failure modes would only show a momentary and hard to detect pressure change. Other detection methods such as flow, liquid level, and current also do not look promising. The following scheme (figure 1) is proposed. Once each hour for a period of three minutes (minute 57, 58, and 59) the hydraulic pressure to the bladder is shut down. This is done by using a clock-driven cam to open a switch that is in series with the torque motor coil. With the hydraulic pressure removed, the captive nitrogen pressure will return to 1100 psi if no nitrogen pressure has been lost due to a leak in the accumulator or a bladder failure. If a failure has occurred, a reed switch in series with the hydraulic pump start-stop relay opens shutting the system down. This switch is a normally open reed switch rotated to the 1100 psi position on a specially modified Bourdon tube pressure gage provided with a magnetic pointer. This switch is by-passed by a second clock-driven cam-activated switch for all but minute 58 of the hourly cycle. It should be noted that the temperature generated by cycling will probably require a pressure set point higher than 1100 psi.

A second reed switch rotated to 1650 psi on the Bourdon tube pressure gage is also in series with the hydraulic pump start-stop relay. If the pressure deviates from the set point of 1650 psi due to power supply, transducer, signal generator, controller, torque motor, servo valve, etc. failure the system will be shut down. This second reed switch is by-passed by a third clock-driven cam-operated switch for minute 56, 57, 58, 59 and 60 of the hourly cycle.

Thus for the first 55 minutes of each hourly cycle the oil pressure side of the bladder is monitored and in the last 5 minutes of each hourly cycle the nitrogen pressure is monitored. If a bladder failure should occur, its time of failure may be known no better than 1 hour which represents 1/2 % of the test period. The output of the strain gage pressure transducer will also be recorded on a slow strip chart recorder.

Other details are shown in figure 1.

At this writing all components have been ordered but delivery schedules are typically quoted at 8-12 weeks.

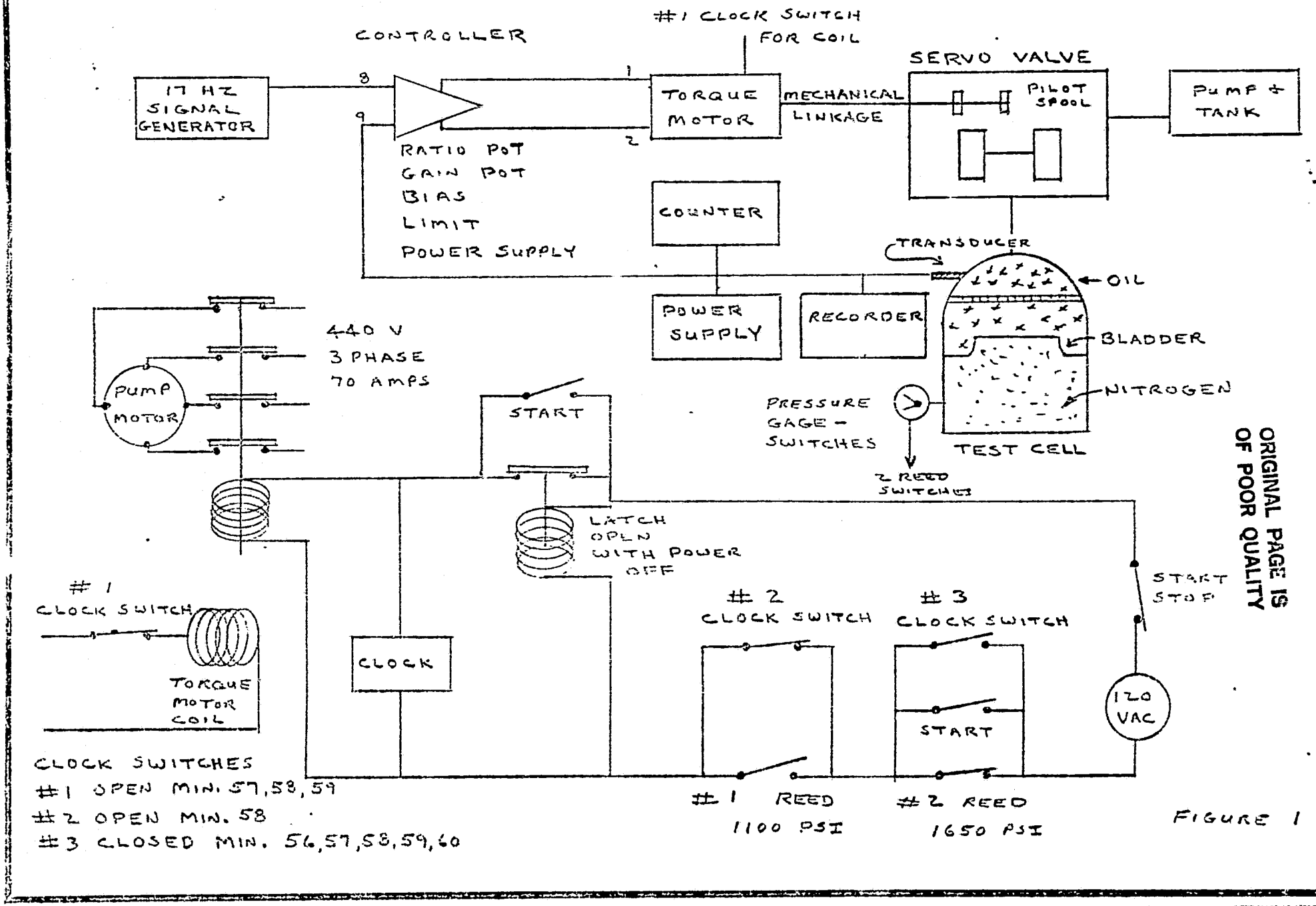

CLOCK SWITCHES
#1 OPEN MIN. 57,58,59
#2 OPEN MIN. 58
#3 CLOSED MIN. 56,57,58,59,60

FIGURE 1

ORIGINAL PAGE IS OF POOR QUALITY

Signal Detection Algorithms in the Search for Extraterrestrial Intelligence

Steven Lord

Department of Physics and Astronomy
University of Massachusetts at Amherst

In efforts to detect radio transmissions from unknown intelligent extra-terrestrial sources, any effective search depends on the employment of sensitive data processing algorithms. In conjunction with the Ames SETI Group Science Team, I have have explored the possibility of using several previously suggested techniques (Drake, '81; Lord, '81) and have suggested some new ones as well.

One established technique, called pseudobinning, is an examination of the output of the Multi-Channel Spectrum Analyser at successively coarser resolutions in hopes of matching the bandwidth of any incomming signal. This summer I assisted by designing digital circuits for this technique, and by exploring theoretical threshhold setting calculations (Drake, ibid.) that prescribe how to achieve a desired false alarm rate using this method under noise conditions. In addition, I developed software algorithms for off-line use of this method, and determined the assembly language version's minimal time budget.

In the two summers I have provided the group with ideas for various alternative algorithms and processing techniques including the block diagrams for a data array (time,frequency) transposition scheme that arranges MCSA data in a more accessible form, followed by cross-correlation processor that serves as a matched filter for on-again, off-again carrier waves. As a "nonspecific signal" type detector, a pattern recognition simulation was written which isolated and highlighted detected signals in noise on a video graphics display. The technique used an adjancency algorithm, which detected the presence of multiple detections closely associated in frequency and/or time.

To prepare for the day when the available detection equipment includes a radiotelescope with dual othogonally polarized receivers, algorithms possessing greatly enhanced sensitivity to polarized signals have been developed (Lord, ibid.), which, by processing the complex output of two MCSAs, dynamically match to the polarization of the incomming signal. The eventual desirability of such coherent detection was discussed and agreed upon by the team, and this technique called generalized coherence, is likely to be the subject of further investigation.

By attempting to determine the sensitivity of various algorithms, especially pseudobinning and coherent detection, I studied the work of Oliver in Drake, ibid. This led me to conclude that there did in fact exist a general way of determining unambigously and objectively the sensitivity of an algorithm.

This method is shown in the figure below. Once the algorithm's response to a known noise spectrum in learned, either by theory or simulation, as well as the algorithm's response to relatively large signal to noise ratio environment, a single sensitivity estimate here called S/N may be obtained for any desired probability of false alarm and probability of missed signal, here represented by Pr_{fa} and Pr_{ms}.

This method can be used to rate two candidate algorithms that may have been designed to respond to the same signal type.

Figure 1.

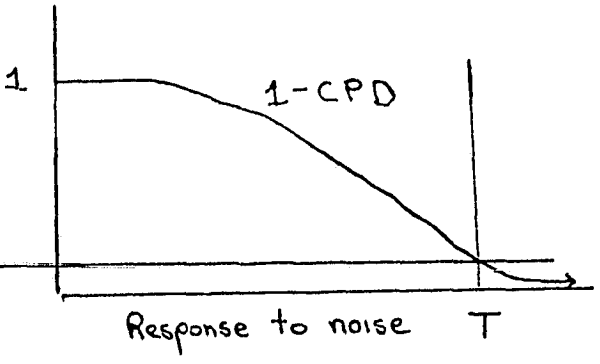

Step 1. Use fixed Pr_{fa} to give T. Here we plot 1 minus the cumulative probability density fuction of the algorithm's response to noise alone. A desired probability of a false alarm yields the threshhold T of the algorithm (the output level at which the algorithm will declare the presence of a signal.)

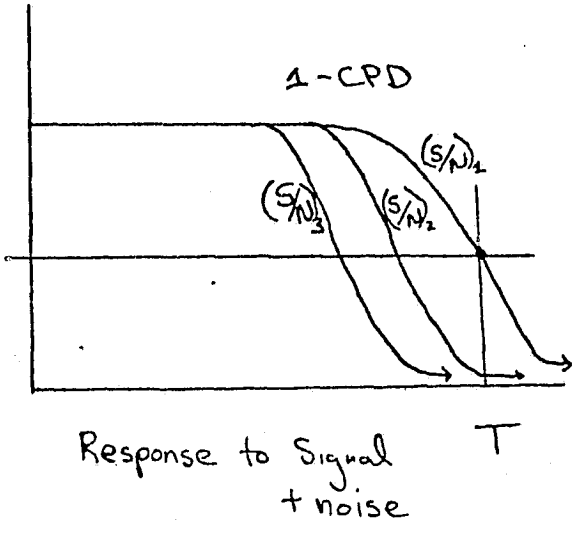

Step 2. We use T and Pr_{ms} to find S/N. Here we plot 1-CPD for various values of S/N input to the algorithm. For a fixed Pr_{ms} there is one S/N curve which passes through the point (T, Pr_{ms}). The S/N_1 value may be thought of as the algorithms sensitivity for the given Pr_{fa} and Pr_{ms} conditions. A lower S/N corresponds to a higher sensitivity.

References:

Drake, F., Wolfe., J., The 1981 Report of the SETI Science Working Group. (Preprint), NASA-Ames Reaserch Center.

Lord, S., Dixon, R., Healy, T., Project Oasis Report, U. of Santa Clara Press, 1981 NASA-ASEE Summer Study Report.

Infrared Spectroscopic Studies of the Effect of Elevated Temperature on the Association of Amino Acids with Clays

John W. Macklin

University of Washington
Department of Chemistry

One of the models associated with origin of life chemistry at Ames involves the enhancement of peptide bond formation between amino acids by heating in the presence of clay minerals. Clay and amino acid mixtures are cycled repeatedly through wet cold and dry hot conditions to achieve increases in oligomer formation of 40 to 200 times that obtained in the absence of clay.[1,2] The explicit chemical mechanism is not known. Recent chemical studies suggest that a covalent type association between the clay and amino acid may constitute the "activated intermediate" that leads to oligomerization.[3] The research described in this report seeks to determine the nature of clay amino acid association at elevated temperatures and elucidate the mechanism for promotion of amino acid oligomerization in the presence of clays.

The experimental approach is to use Fourier transform infrared spectroscopy (FTIR) to measure variations in the vibration spectra of clay-amino acid samples with increasing temperature. Thin, free standing clay films are prepared by evaporation of water from large droplets containing the clay or clay-acid mixture placed on a smoothed sheet of flexible polyethylene. Silica and alumina samples are measured as films on AgCl. Pyroglutamic acid was chosen for these studies because the carboxilate group will have the same character as that of other amino acids but it is not likely to form intermolecular peptide bonds that would displace covalent associations of the carboxilate group with the clay. The clay acid association is thus preserved for observation. The samples are held undisturbed in a heated thermostated cell[4] while spectra are measured at temperatures near 24, 60, 120, 160 and 220°C. The temperature is measured with a chrome-alomel thermocouple near the sample. Spectra taken at lower temperatures are computer substracted from higher temperature measurements to obtain the explicit changes dependant upon increasing the temperature.

Results from one of the experiments are shown in Figure 1. The known temperature dependent variations in the separate spectra of the clay[5] and pyroglutamic acid[6] are accounted for so that variations dependent upon interactions of pyroglutamic acid with the clay can be determined. The experiment has been carried out with several types of clay as well as silica gel alumnia in the form of Gibsite.

A number of intensity variations are consistently observed in the difference spectra of clay-pyroglutamic acid mixtures. For example, note the intensity

increases at about 1200, 1320 and 1780 cm^{-1} and decreases near 700, 1245, 1442 and 1680 cm^{-1} in the measurements shown in Figure 1. The observed changes are consistent with the formation of an ester type association between the pryoglutamic acid carboxyl group and the mineral surface at elevated temperatures. For example, formation of an aceyl silicate may be indicated. We are continuing experiments in order to fully define the meaning of the spectral variations.

My experience as a NASA-ASEE has been most rewarding. I intend to continue my association with NASA colleagues and am formally proposing to contribute to other NASA projects by contractual arrangement.

References

1. N. Lahav, D. White and S. Chang, Science, 201, 67 (1978)
2. D. White, J. Erickson, J. Mol. Evol., 16, 279 (1980)
3. (a) D. Jewett and J. Lawless, Naturwissenchaften, 68, 570 (1981)
   (b) D. White, J. Erickson, private communication, manuscript in preparation.
4. T. Wydeven and M. Leban, Anal. Chem. 39, 1673 (1976)
5. "The Infrared Spectra of Minerals", V. C. Farmer, Chap. 5, pp. 331-64, Mineralogical Society, London (1974)
6. Marino Vitores-Lozano and Anne-Marie Bellocq, J. Chimie Physique, 70, 1337 (1973

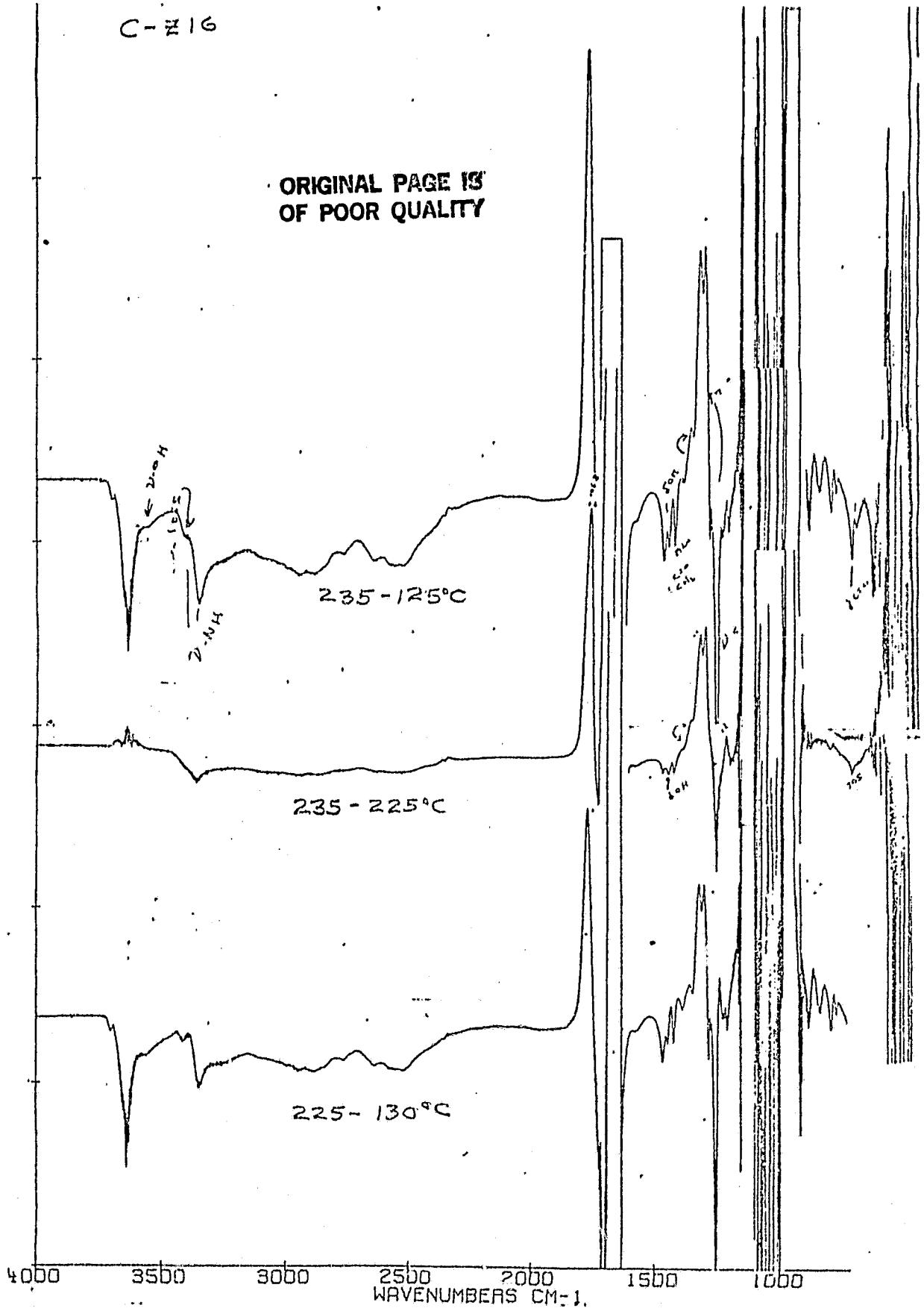

Figure 1. FTIR difference spectra of sodium montmorillonite containing 50% pyroglutamic acid by weight taken at various temperatures. The temperatures at which the spectra included in each subtraction were measured are indicated below each trace.

TITAN'S AEROSOLS

Peter H. Smith

Lunar and Planetary Lab
University of Arizona

Most of the observations of Titan that are now available really "see" the upper haze layers which are known to blanket the entire lower atmosphere and surface. Therefore, when we study Titan with optical methods we are learning about aerosol properties. Although it has been three years since the first flyby mission to Titan, there is still no general concensus as to what the basic properties of the main haze layer, i.e. size, optical constants and pressure levels, are. It was in order to reconcile some of the conflicting results proposed by different groups working in this area that I came to Ames and decided to work with James Pollack.

The observed characteristics of the haze layer are now accepted as follows. Ground-based observations of the geometric albedo reveal an increasing amount of absorption of solar energy toward shorter wavelengths in the blue. This has interpreted as an absorbing haze high in the atmosphere. Voyager I confirmed this hypothesis and placed the haze layer about 250 km above the solid surface. Both the Pioneer and Voyager missions found this haze to be extremely highly polarizing. Tomasko and Smith (1982) interpret this to be evidence that the aerosols are small ($\sim$0.1 μm), dark and that their size increases with depth. Physical models of Titan's aerosols (Toon *et al.*, 1980) also predict this behavior but with larger sizes. Voyager I found a new property: the haze is very forward scattering. Rages *et al.* (1982) explain that the observed forward scattering is indicative of the diffraction from particles of radius greater than 0.19μm and they favor a size nearer 0.5 μm. Voyager II confirms this forward scattering character of the atmosphere leaving investigators in the position of choosing between mutually exclusive models for the haze layer.

My first project this summer at Ames has been to put together the Pioneer and Voyager data sets in such a way as to derive the single scattering properties of an aerosol particle. Normally, these properties serve as the input to an atmosphere model. From a preliminary analysis I've found that the phase function is decidedly non-spherical: forward scattering yet with little back peak and highly polarizing (see Figure). We investigated prolate spheroids last summer (Smith, 1982) with some success. Of course, because other shapes may be more appropriate, we have started a literature search of the various laboratory data pertaining to non-spheres of different classes. Analytical calculations are only possible for spheroids and cylinders.

In analyzing the largest phase angle images this summer, it has become clear that plane parallel atmosphere calculations are inadequate. So to really define the single scattering properties at the most forward scattering geometries, I am collaborating with Kathy Rages who has written a spherical scattering program and can help develop correction factors to boost the intensities calculated from my plane parallel program. We are very close at the end of this summer to a

final definition to the forward peak of the phase function for the atmosphere of haze aerosols and are ready to begin the search phase of our project. I plan to continue this search at the Lunar and Planetary Lab in Tucson and will stay in communication with Pollack and Rages as the project progresses.

In developing the procedures and techniques for analyzing the Titan data it has been useful to exchange ideas with other workers in the field here at Ames. I'm especially indebted to Brian Toon and Morris Podolak, on leave from Tel Aviv.

References

Rages, K.A., Pollack, J.B. and Smith, P.H. (1982). Size estimates of Titan's aersols based on voyager I high phase angle images. (submitted to Icarus).

Smith, P.H. (1982). The case for a bimodal size distribution in Titan's upper haze layer. In The Comparative Study of Planets. (A. Coradini and M. Fulchiguoni, Eds.), pp. 253-260. D. Reidel Publishing Co., Holland.

Tomasko, M.G. and Smith P.H. (1982). Photometry and polarimetry of Titan: Pioneer 11 observations and their implications for aerosol properties. Icarus (in press).

Toon, O.B., Turco, R.P. and Pollack, J.B. (1980). A physical model of Titan's clouds. Icarus, 43, 260-282.